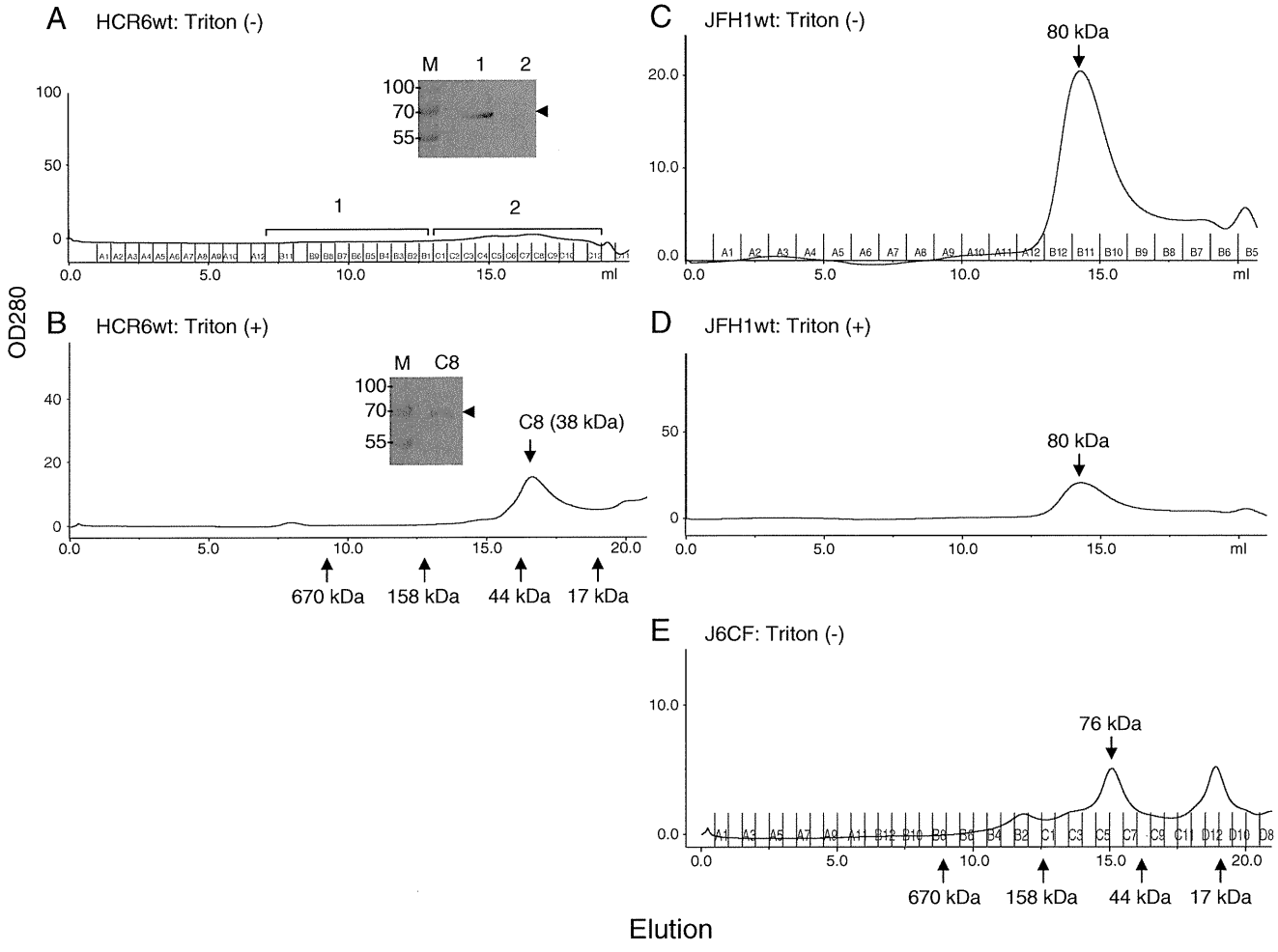

Fig. 5. Superdex 200 gel filtration of HCV HCR6 (1b), JFH1 (2a), and J6CF (2a) wild-type RNA polymerase with or without 0.1% Triton X-100. HCV HCR6 (1b) RdRpwt was applied on Superdex 200 gel filtration columns in 50 mM Tris–HCl (pH 7.5), 150 mM NaCl, 3.5 mM $MnCl_2$, 1 mM DTT, and 0.2% glycerol without (A) or with 0.1% Triton X-100 (B). HCV JFH1 (2a) RdRpwt was applied without (C) or with 0.1% Triton X-100 (D), and J6CF (2a) RdRp was applied without Triton X-100 (E) on the same columns. The elution position of the standard molecular weight markers is indicated below the graph. The molecular weight of the peak fraction is indicated in each graph. Inset in A: The fractions of the void volume—158 kDa (1) and those of lower molecular weight fractions (2) of HCR6 (1b) RdRpwt gel filtration without Triton X-100 were precipitated with TCA and analyzed by western blot. Inset in B: Fraction C8 of HCR6 (1b) RdRpwt with Triton X-100 was precipitated with TCA and analyzed by western blot. The position of HCR6 (1b) RdRpwt is indicated by an arrowhead. The position of the pre-stained size marker is indicated on the left side of the blots.

Km and *Vmax* of HCR6 (1b) RdRp without Triton X-100 for GTP was calculated as $54.7 \pm 3.67\,\mu M$ and 2.52 ± 0.108/min, respectively (Weng et al., 2009).

4. Discussion

Non-ionic (Triton X-100, NP-40, Tween 20, Tween 80, and Brij 35) and twitterionic (CHAPS) detergents activated HCV 1b RdRp by 7.2–16.6 folds when used at their CMC, but did not affect 1a or 2a RdRps (Figs. 1–3, Table 2). In turn, ionic detergents (SDS and DOC) completely inactivated polymerase activity at 0.01%. CMC is the minimum concentration at which a detergent forms micelles; above that concentration, a detergent exists as a large molecular weight complex. The CMC signifies the strength at which a detergent binds to proteins, i.e., low values indicate strong binding, whereas high values indicate weak binding. It is also an indication of the hydrophilicity of a detergent. Triton X-100, NP-40, and Brij 35 at CMC activated Moloney leukemia virus reverse transcriptase by interacting with the hydrophobic domain (Thompson et al., 1972). The activation mechanism of HCV RdRp by these detergents may be similar. However, the detergent interaction domain of HCV RdRp remains to be identified.

Triton X-100 is commonly used for purification of HCV RdRp from the bacteria and insect cells expressing this protein (Lohmann et al., 1997; Luo et al., 2000; Cramer et al., 2006; Weng et al., 2009). HCV 1b RdRp without the C-terminal hydrophobic region expressed in bacteria formed a large molecule complex in 0.1% Triton X-100 or 0.5% CHAPS with a low-salt buffer (<50 mM NaCl) (Qin et al., 2002; Wang et al., 2002). Under low-salt conditions, HCV RdRp was gel filtrated in void volume as a complex with contaminating nucleic acids, because HCV RdRp binds to RNA during purification without high-salt (0.5 M NaCl) stripping (Figs. S1 and S2). Therefore, the presence of HCV 1b RdRp in the void volume fraction of gel filtration by Wang et al. (Wang et al., 2002) could rather represent the complex of HCV RdRp with contaminating nucleic acids. Nevertheless, they also found monomers of HCV 1b RdRp in the gel filtration buffer containing 0.5% CHAPS, which activated polymerase activity (Fig. 1G). Detection of the monomeric HCV 1b RdRps by gel filtration in a buffer containing Triton X-100 and CHAPS has also been reported by other groups (Qin et al., 2002; Wang et al., 2002). HCR6 (1b) RdRpwt formed oligomers in physiological conditions without Triton X-100. In the presence of Triton X-100, HCR6 (1b) RdRpwt was eluted as the monomer which gel-filtration size was smaller than its size in 0.5 M NaCl (Fig. S1D) or calculated from its amino acid composition (64 kDa). HCV 2a (JFH1 and J6CF) RdRps formed a monomer in the same buffer without Triton X-100. Gel filtration analysis of 502 mutants of JFH1 (2a) and HCR6 (1b) RdRps have confirmed that 502H

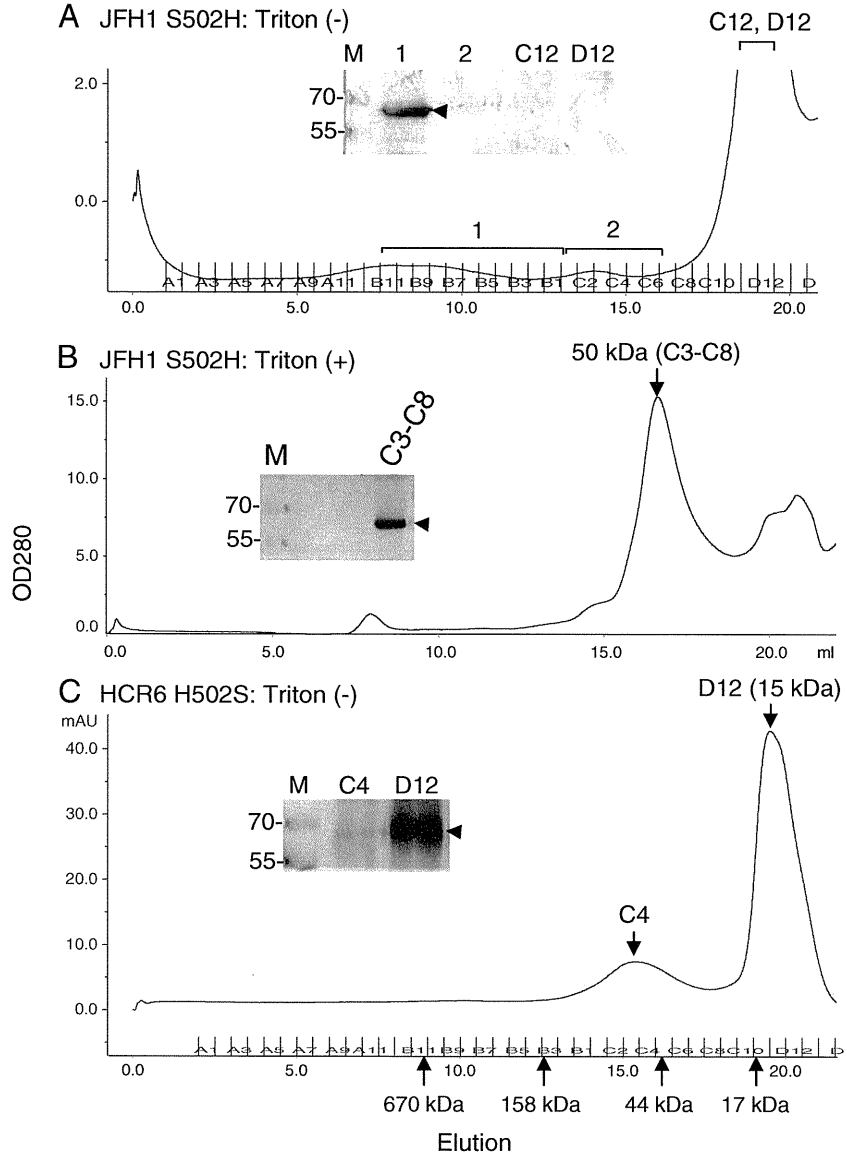

Fig. 6. Superdex 200 gel filtration of HCV JFH1 (2a) and HCR6 (1b) 502 mutant RNA polymerases. JFH1 (2a) S502H (A), and HCR6 (1b) H502S RdRps (C) were applied on Superdex 200 gel filtration columns in 50 mM Tris–HCl (pH 7.5), 150 mM NaCl, 3.5 mM $MnCl_2$, 1 mM DTT, and 0.2% glycerol. JFH1 (2a) RdRpS502H was also applied with 0.1% Triton X-100 (B). Inset in A: The fractions of the void volume—158 kDa (1), those of lower molecular weight fractions (2), fractions C12, and D12 of JFH1 (2a) RdRpS502H gel filtrations were precipitated with TCA and analyzed by western blot. Inset in B: Fraction C3–C8 of JFH1 (2a) RdRpS502H in Triton X-100 were precipitated with TCA and analyzed by western blot. Inset in C: Fractions C4 and D12 of HCR6 (1b) RdRpH502S were precipitated with TCA and analyzed by western blot. The position of HCV RdRp is indicated by an arrowhead. The position of the pre-stained size marker is indicated on the left side of the blots.

is important for the intermolecular interaction of HCV 1b RdRp (Qin et al., 2002). HCV RdRps without the C-terminal hydrophobic domain were soluble in high-salt buffer (>300 mM NaCl; Fig. S1) (Ferrari et al., 1999). The shift to the delayed elution of gel-filtration of HCR6 (1b) RdRpwt and JFH1 (2a) RdRp S502H with Triton X-100, and HCR6 (1b) RdRpH502S may come from the interaction of the RdRps with Superdex200 gel matrix induced by the mutations and Triton X-100.

Our data of HCV RdRp oligomerization at 502H (Fig. 6) are in agreement with those by Qin et al. (Qin et al., 2002), but are contradictory to those obtained by more sensitive methods (fluorescence resonance energy transfer [FRET] and yeast two-hybrid system) (Wang et al., 2002; Clemente-Casares et al., 2011). Interactions between a charged amino acid (His) and an aromatic residue (Trp) (Fernandez-Recio et al., 1997; Matthews et al., 1997; Takeuchi et al., 2003), or His–Glu interactions (Marti and Bosshard, 2003), are often found in proteins. JFH1 (2a) RdRpwt did not form dimers (Chinnaswamy et al., 2010). 502H may interact with 125 W in αF (Clemente-Casares et al., 2011), but not with 18E (Qin et al., 2002). This interaction is dissociated both with high-salt (Fig. S1) and with Triton X-100 (Figs. 5 and 6). Taken together, 502H of HCV 1b RdRp is important for oligomer formation in transcription (physiological salt) conditions. Besides the oligomerization using 502H, the αF and αT helixes of HCV RdRp, which were proposed to be involved in oligomerization (Clemente-Casares et al., 2011), may also be involved in oligomerization of the molecules in transcription condition. The 502 mutations in HCR6 (1b) and JFH1 (2a) RdRps are likely to affect the structure of the template channel by affecting the helix structures of the thumb domain (Bressanelli et al., 2002; Chinnaswamy et al., 2008) because the polymerase and RNA template binding activity of these mutant RdRps was not activated by Triton X-100 (Figs. 3 and 4). These findings indicate the importance around amino acid 502H for HCV 1b RdRp structure. However, these data contradict to the previous reports (Qin et al., 2002; Clemente-Casares et al., 2011).

Comparing the polymerase and template RNA-binding activity of JFH1 (2a) and HCR6 (1b) RdRps with and without Triton X-100,

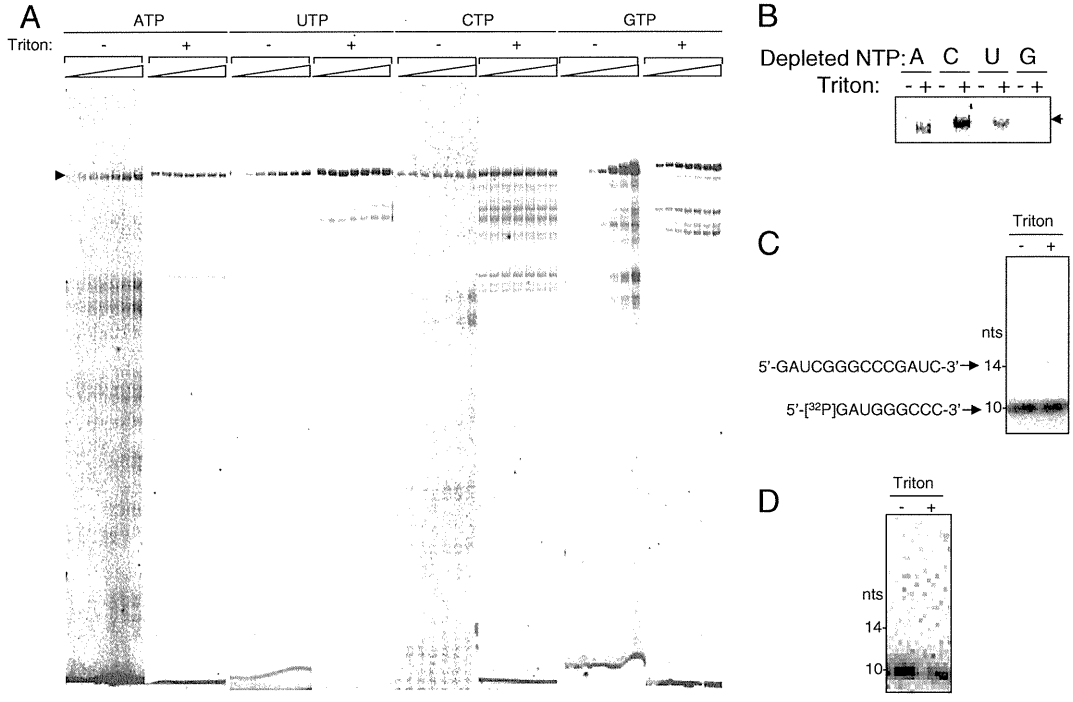

Fig. 7. Effect of substrate concentrations on in vitro transcription of HCR6 (1b) wild-type RNA polymerase, and TNTase activity in the presence of Triton X-100. A: Effect of nucleotide concentration on HCV HCR6 (1b) RdRpwt in vitro transcription with (+) and without (−) 0.02% Triton X-100. The concentration of ATP, UTP, and CTP varied from 1 to 50 μM, and that of GTP varied from 5 to 500 μM. B: Effect of nucleotide depletion on HCV HCR6 (1b) RdRpwt in vitro transcription with (+) and without (−) 0.02% Triton X-100. The position of 184-nt products is indicated by an arrowhead (A and B). C: TNTase activity of HCV HCR6 (1b) RdRpwt. 5′-[^{32}P]sym/sub was transcribed by HCV HCR6 (1b) RdRpwt with (+) and without (−) 0.02% Triton X-100. D: TNTase activity of HCV HCR6 (1b) RdRpwt. sym/sub was transcribed with [^{32}P]UTP by HCV HCR6 (1b) RdRpwt with (+) and without (−) 0.02% Triton X-100. The position of 10-nt sym/sub and 14-nt is indicated on the left.

RdRp which formed oligomer using 502H did not show high polymerase activity (Figs. 3–6). The inactive oligomer may be a part of the reason why a small fraction, less than 1%, of the purified HCV BK RdRp which belonged to 1b participated productively in transcription in vitro (Carroll et al., 2000). Taking together the data obtained by FRET (Clemente-Casares et al., 2011) and yeast two-hybrid systems (Wang et al., 2002), dynamic intermolecular interactions may occur under transcription conditions through the αT helix where amino acid 502 is located. The reason why only 1b RdRp was activated with Triton X-100 although RNA binding of all the RdRps tested was enhanced with Triton X-100, is not clear.

In case of JFH1 (2a) RdRp, the interaction with Triton X-100 may be different from that of HCR6 (1b) RdRp because it was not activated with Triton X-100 (Figs. 1 and 3), and because its gel-filtration profile was not affected with Triton X-100 (Fig. 5). This may be the reason of the inhibition of polymerase activity of JFH1 (2a) RdRpS502H by Triton X-100 although it was also disrupted to monomer (Figs. 3 and 6).

Triton X-100 activated only HCV 1b RdRp (Figs. 3 and 4). The closed conformation of HCV RdRp is required for de novo initiation (Chinnaswamy et al., 2008). With and without Triton X-100, JFH1 (2a) RdRpwt showed as high polymerase activity as HCR6 (1b) RdRpwt did with Triton X-100 (Fig. 3B). The very closed conformation of JFH1 (2a) RdRp is proposed to facilitate de novo initiation and high polymerase activity (Simister et al., 2009). Triton X-100 may also help the conformational change of HCR6 (1b) RdRp to the very closed conformation like that of JFH1 (2a) RdRp during transcription initiation.

HCV RdRp was co-purified with nucleic acids (Figs. S1 and S2). The contaminating nucleic acids were removed from HCV RdRp by high salt treatment. The contaminating nucleic acids carry proteins that have affinity to them, which misleads HCV in vitro transcription data. They also oligomerize HCV RdRp by crosslinking them. In a similar way, the contaminating nucleic acids in HCV RdRp preparations may mislead the binding data of HCV RdRp with other proteins.

From the activation kinetics of the detergents (Fig. 1, Table 1), the polymerase activation of 1b RdRp is likely to depend on the micelle formation of the detergent and on the direct interaction between RdRp and the detergents. The reason why the non-ionic detergent nOG did not activate the HCV RdRp is not known (Figs. 1 and 2).

The interaction mechanism of Triton X-100 and HCV 1b RdRp may be similar as that of sphingomyelin and HCV 1b RdRp because their activation kinetics were similar and the activated genotype was the same (Weng et al., 2010). Sphingomyelin activated only HCV 1b, but did not activate 1a or 2a RdRps. Both the activation curve of sphingomyelin and that of Triton X-100 showed the linear increase of polymerase activity. Then, sphingomyelin reached plateau at 20 molecules, and Triton X-100 reached plateau around its CMC.

Data about TNTase activity of HCV RdRp are controversial (Behrens et al., 1996; Ranjith-Kumar et al., 2001, 2004; Vo et al., 2004). In our system, TNTase activity was not detected with or without Triton X-100 (Figs. 7C and D).

GTP binds to HCV RdRp both as substrate and as a component of RdRp (Bressanelli et al., 2002). The apparent *K*m for GTP with Triton X-100 indicated that the substrate affinity dropped as low as to lose fidelity (Table 1, Figs. 7A and B). Triton X-100 may have affected the substrate-binding although its mechanism is not clear. HCV 1b full-length RdRp transcription activity obtained with CHAPS (Wang et al., 2002) might be that without fidelity as shown with Triton X-100. Detergents should not be used while screening substrate inhibitors of HCV RdRp. These data indicate that caution should be exercised while using detergents in anti-HCV RdRp drug screening tests.

Supplementary materials related to this article can be found online at doi:10.1016/j.gene.2012.01.044.

Acknowledgments

We thank Dr. J. Bukh, Dr. C. Rice, and Dr. R. Bartenshlager for providing pJ6CF, pHCVrepl3(S2204I)Neo, and Con1, respectively. This

work was supported by a Grant-in-Aid from the Chinese Academy of Sciences (O514P51131 and KSCX1-YW-10), the Chinese 973 Project (2009CB522504), and the Chinese National Science and Technology Major Project (2008ZX10002-014).

References

Aizaki, H., Lee, K.J., Sung, V.M., Ishiko, H., Lai, M.M., 2004. Characterization of the hepatitis C virus RNA replication complex associated with lipid rafts. Virology 324, 450–461.

Arnold, J.J., Cameron, C.E., 2000. Poliovirus RNA-dependent RNA polymerase (3D(pol)). Assembly of stable, elongation-competent complexes by using a symmetrical primer-template substrate (sym/sub). J. Biol. Chem. 275, 5329–5336.

Behrens, S.E., Tomei, L., De Francesco, R., 1996. Identification and properties of the RNA-dependent RNA polymerase of hepatitis C virus. EMBO J. 15, 12–22.

Binder, M., Quinkert, D., Bochkarova, O., Klein, R., Kezmic, N., Bartenschlager, R., Lohmann, V., 2007. Identification of determinants involved in initiation of hepatitis C virus RNA synthesis by using intergenotypic replicase chimeras. J. Virol. 81, 5270–5283.

Blight, K.J., McKeating, J.A., Marcotrigiano, J., Rice, C.M., 2003. Efficient replication of hepatitis C virus genotype 1a RNAs in cell culture. J. Virol. 77, 3181–3190.

Bressanelli, S., Tomei, L., Rey, F.A., De Francesco, R., 2002. Structural analysis of the hepatitis C virus RNA polymerase in complex with ribonucleotides. J. Virol. 76, 3482–3492.

Carroll, S.S., Sardana, V., Yang, Z., Jacobs, A.R., Mizenko, C., Hall, D., Hill, L., Zugay-Murphy, J., Kuo, L.C., 2000. Only a small fraction of purified hepatitis C RNA-dependent RNA polymerase is catalytically competent: implications for viral replication and in vitro assays. Biochemistry 39, 8243–8249.

Chinnaswamy, S., Murali, A., Li, P., Fujisaki, K., Kao, C.C., 2010. Regulation of de novo-initiated RNA synthesis in hepatitis C virus RNA-dependent RNA polymerase by intermolecular interactions. J. Virol. 84, 5923–5935.

Chinnaswamy, S., Yarbrough, I., Palaninathan, S., Kumar, C.T., Vijayaraghavan, V., Demeler, B., Lemon, S.M., Sacchettini, J.C., Kao, C.C., 2008. A locking mechanism regulates RNA synthesis and host protein interaction by the hepatitis C virus polymerase. J. Biol. Chem. 283, 20535–20546.

Clemente-Casares, P., Lopez-Jimenez, A.J., Bellon-Echeverria, I., Encinar, J.A., Martinez-Alfaro, E., Perez-Flores, R., Mas, A., 2011. De novo polymerase activity and oligomerization of hepatitis C virus RNA-dependent RNA-polymerases from genotypes 1 to 5. PLoS One 6, e18515.

Cramer, J., Jaeger, J., Restle, T., 2006. Biochemical and pre-steady-state kinetic characterization of the hepatitis C virus RNA polymerase (NS5BDelta21, HC-J4). Biochemistry 45, 3610–3619.

Fernandez-Recio, J., Vazquez, A., Civera, C., Sevilla, P., Sancho, J., 1997. The tryptophan/histidine interaction in alpha-helices. J. Mol. Biol. 267, 184–197.

Ferrari, E., Wright-Minogue, J., Fang, J.W., Baroudy, B.M., Lau, J.Y., Hong, Z., 1999. Characterization of soluble hepatitis C virus RNA-dependent RNA polymerase expressed in *Escherichia coli*. J. Virol. 73, 1649–1654.

Grakoui, A., McCourt, D.W., Wychowski, C., Feinstone, S.M., Rice, C.M., 1993. Characterization of the hepatitis C virus-encoded serine proteinase: determination of proteinase-dependent polyprotein cleavage sites. J. Virol. 67, 2832–2843.

Hijikata, M., Mizushima, H., Tanji, Y., Komoda, Y., Hirowatari, Y., Akagi, T., Kato, N., Kimura, K., Shimotohno, K., 1993. Proteolytic processing and membrane association of putative nonstructural proteins of hepatitis C virus. Proc. Natl. Acad. Sci. U. S. A. 90, 10773–10777.

Hirschman, S.Z., Gerber, M., Garfinkel, E., 1978. Differential activation of hepatitis B DNA polymerase by detergent and salt. J. Med. Virol. 2, 61–76.

Hong, Z., Cameron, C.E., Walker, M.P., Castro, C., Yao, N., Lau, J.Y., Zhong, W., 2001. A novel mechanism to ensure terminal initiation by hepatitis C virus NS5B polymerase. Virology 285, 6–11.

Kashiwagi, T., Hara, K., Kohara, M., Iwahashi, J., Hamada, N., Honda-Yoshino, H., Toyoda, T., 2002a. Promoter/origin structure of the complementary strand of hepatitis C virus genome. J. Biol. Chem. 277, 28700–28705.

Kashiwagi, T., Hara, K., Kohara, M., Kohara, K., Iwahashi, J., Hamada, N., Yoshino, H., Toyoda, T., 2002b. Kinetic analysis of C-terminally truncated RNA-dependent RNA polymerase of hepatitis C virus. Biochem. Biophys. Res. Commun. 290, 1188–1194.

Kiyosawa, K., Sodeyama, T., Tanaka, E., Gibo, Y., Yoshizawa, K., Nakano, Y., Furuta, S., Akahane, Y., Nishioka, K., Purcell, R.H., et al., 1990. Interrelationship of blood transfusion, non-A, non-B hepatitis and hepatocellular carcinoma: analysis by detection of antibody to hepatitis C virus. Hepatology 12, 671–675.

Lemon, S., Walker, C., Alter, M., Yi, M., 2007. Hepatitis C virus. In: Knipe, D., Howley, P. (Eds.), *Fields Virology*. Lippincott-Raven Publishers, Philadelphia, PA, pp. 1253–1304.

Lohmann, V., Korner, F., Herian, U., Bartenschlager, R., 1997. Biochemical properties of hepatitis C virus NS5B RNA-dependent RNA polymerase and identification of amino acid sequence motifs essential for enzymatic activity. J. Virol. 71, 8416–8428.

Luo, G., Hamatake, R.K., Mathis, D.M., Racela, J., Rigat, K.L., Lemm, J., Colonno, R.J. De, 2000. novo initiation of RNA synthesis by the RNA-dependent RNA polymerase (NS5B) of hepatitis C virus. J. Virol. 74, 851–863.

Marti, D.N., Bosshard, H.R., 2003. Electrostatic interactions in leucine zippers: thermodynamic analysis of the contributions of Glu and His residues and the effect of mutating salt bridges. J. Mol. Biol. 330, 621–637.

Matthews, J.M., Ward, L.D., Hammacher, A., Norton, R.S., Simpson, R.J., 1997. Roles of histidine 31 and tryptophan 34 in the structure, self-association, and folding of murine interleukin-6. Biochemistry 36, 6187–6196.

Murayama, A., Date, T., Morikawa, K., Akazawa, D., Miyamoto, M., Kaga, M., Ishii, K., Suzuki, T., Kato, T., Mizokami, M., Wakita, T., 2007. The NS3 helicase and NS5B-to-3′X regions are important for efficient hepatitis C virus strain JFH-1 replication in Huh7 cells. J. Virol. 81, 8030–8040.

Murayama, A., Weng, L., Date, T., Akazawa, D., Tian, X., Suzuki, T., Kato, T., Tanaka, Y., Mizokami, M., Wakita, T., Toyoda, T., 2010. RNA polymerase activity and specific RNA structure are required for efficient HCV replication in cultured cells. PLoS Pathog. 6, e1000885.

Qin, W., Luo, H., Nomura, T., Hayashi, N., Yamashita, T., Murakami, S., 2002. Oligomeric interaction of hepatitis C virus NS5B is critical for catalytic activity of RNA-dependent RNA polymerase. J. Biol. Chem. 277, 2132–2137.

Ranjith-Kumar, C.T., Gajewski, J., Gutshall, L., Maley, D., Sarisky, R.T., Kao, C.C., 2001. Terminal nucleotidyl transferase activity of recombinant Flaviviridae RNA-dependent RNA polymerases: implication for viral RNA synthesis. J. Virol. 75, 8615–8623.

Ranjith-Kumar, C.T., Sarisky, R.T., Gutshall, L., Thomson, M., Kao, C.C. De, 2004. novo initiation pocket mutations have multiple effects on hepatitis C virus RNA-dependent RNA polymerase activities. J. Virol. 78, 12207–12217.

Saito, I., Miyamura, T., Ohbayashi, A., Harada, H., Katayama, T., Kikuchi, S., Watanabe, Y., Koi, S., Onji, M., Ohta, Y., et al., 1990. Hepatitis C virus infection is associated with the development of hepatocellular carcinoma. Proc. Natl. Acad. Sci. U. S. A. 87, 6547–6549.

Sakamoto, H., Okamoto, K., Aoki, M., Kato, H., Katsume, A., Ohta, A., Tsukuda, T., Shimma, N., Aoki, Y., Arisawa, M., Kohara, M., Sudoh, M., 2005. Host sphingolipid biosynthesis as a target for hepatitis C virus therapy. Nat. Chem. Biol. 1, 333–337.

Schmitt, M., Scrima, N., Radujkovic, D., Caillet-Saguy, C., Simister, P.C., Friebe, P., Wicht, O., Klein, R., Bartenschlager, R., Lohmann, V., Bressanelli, S., 2011. A comprehensive structure–function comparison of hepatitis C virus strain JFH1 and J6 polymerases reveals a key residue stimulating replication in cell culture across genotypes. J. Virol. 85, 2565–2581.

Shi, S.T., Lee, K.J., Aizaki, H., Hwang, S.B., Lai, M.M., 2003. Hepatitis C virus RNA replication occurs on a detergent-resistant membrane that cofractionates with caveolin-2. J. Virol. 77, 4160–4168.

Simister, P., Schmitt, M., Geitmann, M., Wicht, O., Danielson, U.H., Klein, R., Bressanelli, S., Lohmann, V., 2009. Structural and functional analysis of hepatitis C virus strain JFH1 polymerase. J. Virol. 83, 11926–11939.

Takeuchi, H., Okada, A., Miura, T., 2003. Roles of the histidine and tryptophan side chains in the M2 proton channel from influenza A virus. FEBS Lett. 552, 35–38.

Tanaka, T., Kato, N., Cho, M.J., Sugiyama, K., Shimotohno, K., 1996. Structure of the 3′ terminus of the hepatitis C virus genome. J. Virol. 70, 3307–3312.

Thompson, F.M., Libertini, L.J., Joss, U.R., Calvin, M., 1972. Detergent effects on a reverse transcriptase activity and on inhibition by rifamycin derivatives. Science 178, 505–507.

Tsukiyama-Kohara, K., Iizuka, N., Kohara, M., Nomoto, A., 1992. Internal ribosome entry site within hepatitis C virus RNA. J. Virol. 66, 1476–1483.

Vo, N.V., Tuler, J.R., Lai, M.M., 2004. Enzymatic characterization of the full-length and C-terminally truncated hepatitis C virus RNA polymerases: function of the last 21 amino acids of the C terminus in template binding and RNA synthesis. Biochemistry 43, 10579–10591.

Wang, Q.M., Hockman, M.A., Staschke, K., Johnson, R.B., Case, K.A., Lu, J., Parsons, S., Zhang, F., Rathnachalam, R., Kirkegaard, K., Colacino, J.M., 2002. Oligomerization and cooperative RNA synthesis activity of hepatitis C virus RNA-dependent RNA polymerase. J. Virol. 76, 3865–3872.

Wasley, A., Alter, M.J., 2000. Epidemiology of hepatitis C: geographic differences and temporal trends. Semin. Liver Dis. 20, 1–16.

Watashi, K., Ishii, N., Hijikata, M., Inoue, D., Murata, T., Miyanari, Y., Shimotohno, K., 2005. Cyclophilin B is a functional regulator of hepatitis C virus RNA polymerase. Mol. Cell 19, 111–122.

Weng, L., Du, J., Zhou, J., Ding, J., Wakita, T., Kohara, M., Toyoda, T., 2009. Modification of hepatitis C virus 1b RNA polymerase to make a highly active JFH1-type polymerase by mutation of the thumb domain. Arch. Virol. 154, 765–773.

Weng, L., Hirata, Y., Arai, M., Kohara, M., Wakita, T., Watashi, K., Shimotohno, K., He, Y., Zhong, J., Toyoda, T., 2010. Sphingomyelin activates hepatitis C virus RNA polymerase in a genotype specific manner. J. Virol. 84, 11761–11770.

Weyant, R.S., Edmonds, P., Swaminathan, B., 1990. Effect of ionic and nonionic detergents on the Taq polymerase. Biotechniques 9, 308–309.

Wu, A.M., Cetta, A., 1975. On the stimulation of viral DNA polymerase activity by nonionic detergent. Biochemistry 14, 789–795.

JVI
Journals.ASM.org

Production of Infectious Chimeric Hepatitis C Virus Genotype 2b Harboring Minimal Regions of JFH-1

Asako Murayama,[a] Takanobu Kato,[a] Daisuke Akazawa,[a] Nao Sugiyama,[a] Tomoko Date,[a] Takahiro Masaki,[a] Shingo Nakamoto,[b] Yasuhito Tanaka,[c] Masashi Mizokami,[d] Osamu Yokosuka,[b] Akio Nomoto,[e]* and Takaji Wakita[a]

Department of Virology II, National Institute of Infectious Diseases, Shinjuku-ku, Tokyo, Japan[a]; Department of Medicine and Clinical Oncology, Graduate School of Medicine, Chiba University, Chuo, Chiba, Japan[b]; Department of Virology and Liver Unit, Nagoya City University Graduate School of Medical Sciences, Kawasumi, Mizuho, Nagoya, Japan[c]; The Research Center for Hepatitis and Immunology, National Center for Global Health and Medicine, Ichikawa, Chiba, Japan[d]; and Department of Microbiology, Graduate School of Medicine, University of Tokyo, Bunkyo-ku, Tokyo, Japan[e]

To establish a cell culture system for chimeric hepatitis C virus (HCV) genotype 2b, we prepared a chimeric construct harboring the 5′ untranslated region (UTR) to the E2 region of the MA strain (genotype 2b) and the region of p7 to the 3′ UTR of the JFH-1 strain (genotype 2a). This chimeric RNA (MA/JFH-1.1) replicated and produced infectious virus in Huh7.5.1 cells. Replacement of the 5′ UTR of this chimera with that from JFH-1 (MA/JFH-1.2) enhanced virus production, but infectivity remained low. In a long-term follow-up study, we identified a cell culture-adaptive mutation in the core region (R167G) and found that it enhanced virus assembly. We previously reported that the NS3 helicase (N3H) and the region of NS5B to 3′ X (N5BX) of JFH-1 enabled replication of the J6CF strain (genotype 2a), which could not replicate in cells. To reduce JFH-1 content in MA/JFH-1.2, we produced a chimeric viral genome for MA harboring the N3H and N5BX regions of JFH-1, combined with a JFH-1 5′ UTR replacement and the R167G mutation (MA/N3H+N5BX-JFH1/R167G). This chimeric RNA replicated efficiently, but virus production was low. After the introduction of four additional cell culture-adaptive mutations, MA/N3H+N5BX-JFH1/5am produced infectious virus efficiently. Using this chimeric virus harboring minimal regions of JFH-1, we analyzed interferon sensitivity and found that this chimeric virus was more sensitive to interferon than JFH-1 and another chimeric virus containing more regions from JFH-1 (MA/JFH-1.2/R167G). In conclusion, we established an HCV genotype 2b cell culture system using a chimeric genome harboring minimal regions of JFH-1. This cell culture system may be useful for characterizing genotype 2b viruses and developing antiviral strategies.

Hepatitis C virus (HCV) is a major cause of chronic liver disease (5, 13), but the lack of a robust cell culture system to produce virus particles has hampered the progress of HCV research (2). Although the development of a subgenomic replicon system has enabled research into HCV RNA replication (15), infectious virus particle production has not been possible. Recently, an HCV cell culture system was developed using a genotype 2a strain, JFH-1, cloned from a fulminant hepatitis patient (14, 29, 32), thereby allowing investigation of the entire life cycle of this virus. However, several groups of investigators have reported genotype- and/or strain-dependent effects of some antiviral reagents (6, 17) and neutralizing antibodies (7, 25). Therefore, efficient virus production systems using various genotypes and strains are indispensable for HCV research and the development of antiviral strategies.

The JFH-1 strain is the first HCV strain that can efficiently produce HCV particles in HuH-7 cells (29). Other strains can replicate and produce infectious virus by HCV RNA transfection, but the efficiency is far lower than that of JFH-1 (24, 31). In the case of replication-incompetent strains, chimeric virus containing the JFH-1 nonstructural protein coding region is useful for analyses of viral characteristics (6, 9, 14, 23, 30, 31).

In this study, we developed a genotype 2b chimeric infectious virus production system using the MA strain (accession number AB030907) (19) harboring minimal regions of JFH-1 and cell culture-adaptive mutations that enhance infectious virus production.

MATERIALS AND METHODS

Cell culture. Huh7.5.1 cells (a kind gift from Francis V. Chisari) (32) and Huh7-25 cells (1) were cultured at 37°C in Dulbecco's modified Eagle's medium containing 10% fetal bovine serum under 5% CO_2 conditions. For follow-up study, RNA-transfected cells were passaged every 2 to 5 days depending on cell status.

Full-length genomic HCV constructs. Plasmids used in the analysis of genomic RNA replication were constructed based on pJFH1 (29) and pMA (19). For convenience, an EcoRI recognition site was introduced upstream of the T7 promoter region of pMA by PCR, and an XbaI recognition site was introduced at the end of the 3′ untranslated region (UTR). To construct MA/JFH-1, the EcoRI-BsaBI (nucleotides [nt] 1 to 2570; 5′ UTR to E2) fragment of pMA was substituted into pJFH1 (Fig. 1A). Replacement of the 5′ UTR was performed by exchanging the EcoRI-AgeI (nt 1 to 159) fragment. A point mutation in the core region (R167G) was introduced into MA chimeric constructs by PCR using the following primers: sense, 5′-TTA TGC AAC GGG GAA TTT ACC CGG TTG CTC T-3′; antisense, 5′-GGT AAA TTC CCC GTT GCA TAA TTT ATC CCG TC-3′. G167R substitution in the JFH-1 construct was performed by PCR using the following primers: sense, 5′-ATT ATG CAA CAA GGA ACC TAC CCG GTT TCC C-3′; antisense, 5′-GGT AGG TTC CTT GTT GCA TAA TTA ACC CCG TC-3′. Point mutations (L814S, R1012G, T1106A, and V1951A) were introduced into MA chimeric constructs by PCR using the following primers: L814S, 5′-GCT TAC GCC TCG GAC GCC GCT GAA CAA GGG G-3′ (sense) and 5′-AGC GGC GTC CGA GGC GTA AGC CTG CTG CGG C-3′ (antisense); R1012G, 5′-GAG GCT AGG TGG

Received 13 June 2011 Accepted 23 November 2011
Published ahead of print 7 December 2011
Address correspondence to Takaji Wakita, wakita@nih.go.jp.
* Present address: Institute of Microbial Chemistry, Shinagawa-ku, Tokyo, Japan.

doi:10.1128/JVI.05386-11

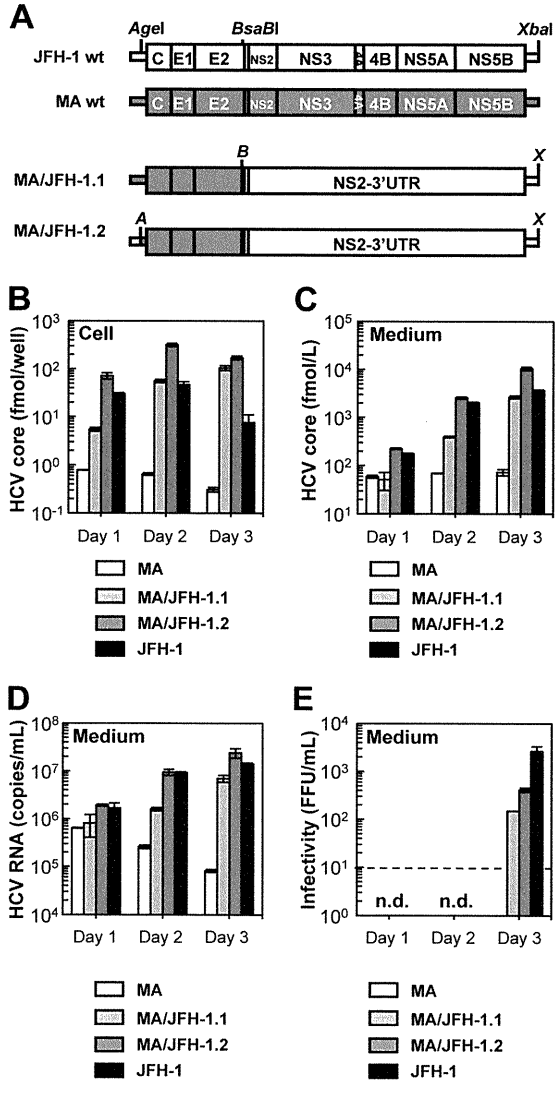

FIG 1 Replication and virus production by MA/JFH-1 chimeras in Huh7.5.1 cells. (A) Schematic structures of JFH-1, MA, and two MA/JFH-1 chimeras (MA/JFH-1.1 and MA/JFH-1.2). The junction of JFH-1 and MA in the 5′ UTR is an AgeI site, and the junction of MA and JFH-1 in the NS2 region is a BsaBI site. A, AgeI; B, BsaBI; X, XbaI. (B to E) Chimeric HCV RNA replication in Huh7.5.1 cells. HCV core protein level in cells (B) and culture medium (C) and HCV RNA levels in medium (D) and infectivity of culture medium (E) from HCV RNA-transfected Huh7.5.1 cells are shown. Ten micrograms of HCV RNA was transfected into Huh7.5.1 cells, and cells and culture medium were harvested on days 1, 2, and 3. n.d., not determined. Assays were performed three times independently, and data are presented as means ± standard deviation. Dashed line indicates detection limit. wt, wild type.

GGA AGT TCT GCT CGG CCC T-3′ (sense) and 5′-AGA ACT TCC CCA CCT AGC CTC GCG GAA ACC G-3′ (antisense); T1106A, 5′-CAG ATG TAC GCC AGC GCA GAG GGG GAC CTC-3′ (sense) and 5′-CTG CGC TGG CGT ACA TCT GGG TGA CTG GTC-3′ (antisense); and V1951A, 5′-GTG ACG CAG GCG TTA AGC TCA CTC ACA ATT ACC-3′ (sense) and 5′-TGA GCT TAA CGC CTG CGT CAC GCG CAG CGA G-3′ (antisense). To construct the MA chimeric virus harboring minimal regions of JFH-1 (MA/N3H+N5BX-JFH1), ClaI (nt 3930), EcoT22I (nt 5294), and BsrGI (nt 7782) recognition sites were introduced into pMA by site-directed mutagenesis. The 5′ UTR (EcoRI-AgeI), the region of the NS3 helicase (N3H; ClaI-EcoT22I), and the region of NS5B to 3′ X (N5BX; BsrGI-XbaI) were then replaced with the corresponding regions from JFH-1.

RNA synthesis, transfection, and determination of infectivity. RNA synthesis and transfection were performed as described previously (12, 22). Determination of infectivity was also performed as described previously, with infectivity expressed as the number of focus-forming units per milliliter (FFU/ml) (12, 22). When necessary, culture medium was concentrated 20-fold in Amicon Ultra-15 spin columns (100-kDa molecular-weight-cutoff; Millipore, Bedford, MA) in order to determine infectivity.

Quantification of HCV core protein and HCV RNA. In order to estimate the concentration of HCV core protein in culture medium, we performed a chemiluminescence enzyme immunoassay (Lumipulse II HCV core assay; Fujirebio, Tokyo, Japan) in accordance with the manufacturer's instructions. HCV RNA from harvested cells or culture medium was isolated using an RNeasy Mini RNA kit (Qiagen, Tokyo, Japan) or QiaAmp Viral RNA Minikit (Qiagen), respectively. Copy number of HCV RNA was determined by real-time quantitative reverse transcription-PCR (qRT-PCR), as described previously (28).

HCV sequencing. Total RNA in culture supernatant was extracted with Isogen-LS (Nippon Gene Co., Ltd., Tokyo, Japan). cDNA was synthesized using Superscript III Reverse Transcriptase (Invitrogen, Carlsbad, CA). cDNA was subsequently amplified with LA *Taq* DNA polymerase (TaKaRa, Shiga, Japan). Four separate PCR primer sets were used to amplify the fragments of nt 130 to 2909, 2558 to 5142, 4784 to 7279, and 7081 to 9634 covering the entire open reading frame and part of the 5′ UTR and 3′ UTR of the MA strain. Sequences of amplified fragments were determined directly.

Immunostaining. Infected cells were cultured on Multitest Slides (MP Biomedicals, Aurora, OH) and were fixed in acetone-methanol (1:1, vol/vol) for 15 min at −20°C. After a blocking step, infected cells were visualized with anti-core protein antibody (clone 2H9) (29) and Alexa Fluor 488 goat anti-mouse IgG (Invitrogen), and nuclei were visualized with 4′,6′-diamidino-2-phenylindole (DAPI).

Assessment of interferon sensitivity. Two micrograms of *in vitro* transcribed RNA was transfected into 3×10^6 Huh7.5.1 cells. Four hours after transfection, cells were placed in fresh medium or medium containing 0.1, 1, 10, 100, and 1,000 IU/ml of interferon α-2b (Intron A; Schering-Plough Corporation, Osaka, Japan). Culture medium was then harvested on day 3, and HCV core levels in the cells and in the medium were measured.

Statistical analysis. Significant differences were evaluated by Student's *t* test. A *P* value of <0.05 was considered significant.

RESULTS

Transient replication and production of 2b/2a chimeric virus. We first tested whether the MA strain (genotype 2b) (19) was able to replicate and produce infectious virus in cultured cells. When the *in vitro* transcribed RNA of MA was transfected into Huh7.5.1 cells, a highly HCV-permissive cell line, replication and virus production were not observed (Fig. 1A to C). We then tested whether 2b/2a chimeric RNA harboring the structural region (5′ UTR to E2) of the MA strain and the nonstructural region (p7 to 3′ UTR) of JFH-1 (Fig. 1A, MA/JFH-1.1) was able to replicate in the cells. After MA/JFH-1.1 RNA transfection, time-dependent accumulation of core protein in the cells (Fig. 1B) and culture medium (Fig. 1C) was observed, indicating that MA/JFH-1.1 RNA was able to replicate in the cells autonomously. HCV RNA levels in the medium were determined by qRT-PCR, and time-dependent increases in HCV RNA level were also observed (Fig. 1D). Infectious virus production was observed on day 3, but infectivity was 17.6-fold lower than that of JFH-1 (Fig. 1E).

In order to improve the level of infectious virus production, we tested another chimeric construct, MA/JFH-1.2, which contained an additional MA-to-JFH-1 replacement of the 5′ UTR (Fig. 1A),

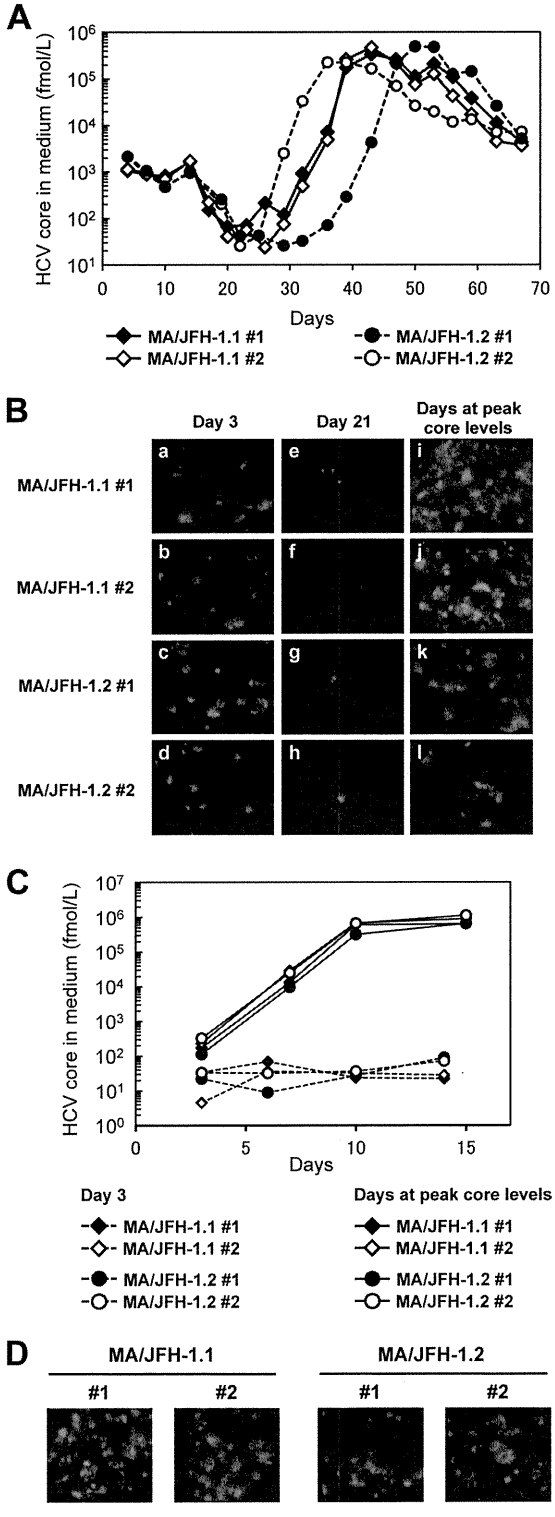

FIG 2 Long-term culture of MA/JFH-1.1 and MA/JFH-1.2 RNA-transfected cells. Ten micrograms of HCV RNA was transfected into Huh7.5.1 cells, and cells were passaged every 2 to 5 days, depending on cell status. Culture medium was collected after every passage, and HCV core protein levels were measured. Transfection was performed twice for each chimeric RNA (1 and 2 for each construct). (A) HCV core protein levels in culture medium from MA/JFH-1.1 and MA/JFH-1.2 RNA-transfected cells. (B) Immunostained cells at 3 days after transfection (a to d), at 21 days after transfection (e to h), and at the time of peak core levels (days 42 to 49). Infected cells were visualized with anti-core protein antibody (green), and nuclei were visualized with DAPI (blue). (C) Infection of naïve cells by culture medium at an MOI of 0.001. (D) Immunostained cells at 15 days after infection with medium at peak core protein levels (Fig. 2A) at an MOI of 0.001. Infected cells were visualized with anti-core antibody (green), and nuclei were visualized with DAPI (blue).

TABLE 1 HCV core protein levels and infectivity in culture medium immediately after RNA transfection (day 3) and after long-term culture (days 35 to 49)

Sample period and virus	Sample no.	Day no.[a]	HCV core (fmol/liter)	Infectivity (FFU/ml)
After transfection				
MA/JFH-1.1	1	3	1.06×10^3	5.00×10^1
	2	3	1.14×10^3	5.70×10^1
MA/JFH-1.2	1	3	2.14×10^3	7.30×10^1
	2	3	2.15×10^3	9.30×10^1
After long-term culture				
MA/JFH-1.1	1	42	3.38×10^5	1.62×10^5
	2	42	4.70×10^5	3.23×10^5
MA/JFH-1.2	1	35	2.27×10^5	1.61×10^5
	2	49	4.93×10^5	3.27×10^5

[a] For the long-term culture, the days are those of peak core protein levels.

as a 5′ UTR replacement from J6CF (genotype 2a) to JFH-1 enhanced virus production of chimeric J6CF virus harboring the region of NS2 to 3′ X of JFH-1 (J6/JFH-1) (A. Murayama et al., unpublished data). The core protein accumulation levels with MA/JFH-1.2 RNA-transfected cells were higher than those with MA/JFH-1.1 ($P < 0.05$) (Fig. 1B). Similarly, core protein and HCV RNA levels in the medium of MA/JFH-1.2 RNA-transfected cells were higher than those of MA/JFH-1.1 ($P < 0.05$) (Fig. 1C and D). Infectivity on day 3 was also higher than with MA/JFH-1.1 ($P < 0.05$) (Fig. 1E), indicating that the 5′ UTR of JFH-1 enhanced virus production. However, infectivity of medium from MA/JFH-1.2 RNA-transfected cells on day 3 remained 6.4-fold lower than that of JFH-1 although HCV RNA levels in the medium were similar to those of JFH-1 (Fig. 1D and E).

These results indicate that 2b/2a chimeric RNA is able to replicate autonomously in Huh7.5.1 cells and produce infectious virus although infectivity remains lower than that of JFH-1.

Assembly-enhancing mutation in core region introduced during long-term culture. Because MA/JFH-1.1 and MA/JFH-1.2 replicated efficiently but produced small amounts of infectious virus, we performed long-term culture of these RNA-transfected cells in order to examine whether these chimeric RNAs would continue replicating and producing infectious virus over the long term. We prepared two RNA-transfected cell lines for each construct (MA/JFH-1.1 and MA/JFH-1.2) as both of these replicated and produced infectious virus at different levels.

Immediately after transfection, core protein levels and infectivity in culture medium were low (1.06×10^3 to 2.15×10^3 fmol/liter and 5.00×10^1 to 9.30×10^1 FFU/ml, respectively) (Fig. 2A and Table 1) although a considerable number of core protein-positive cells were observed by immunostaining (Fig. 2B, frames a to d). Subsequently, core protein levels in the culture medium decreased gradually (Fig. 2A), and core protein-positive cells were rare (Fig. 2B, frames e to h). However, at 30 to 40 days

after transfection, core protein levels in the supernatants of all chimeric RNA-transfected cells increased and reached 2.27×10^5 to 4.93×10^5 fmol/liter (Fig. 2A and Table 1). Infectivity in the culture medium also increased (1.61×10^5 to 3.27×10^5 FFU/ml) (Table 1), and at this point, most of the cells were core protein positive (Fig. 2B, frame i to l).

As the infectivity of culture supernatant of MA/JFH-1 RNA-transfected cells appeared to increase after long-term culture, we compared viral spread by infection with these supernatants on day 3 (immediately after transfection) and for each peak in core protein levels (after long-term culture). When naïve Huh7.5.1 cells were infected with supernatant on days corresponding to a peak in core protein levels at a multiplicity of infection (MOI) of 0.001, core protein levels in the medium increased rapidly and reached 0.64×10^6 to 1.13×10^6 fmol/liter by day 15 after infection (Fig. 2C). Immunostained images showed that most cells were HCV core protein positive on day 15 (Fig. 2D). When naïve Huh7.5.1 cells were infected with supernatant from day 3 at an MOI of 0.001, core protein levels in the medium did not increase under these conditions (Fig. 2C). These results indicate that both MA/JFH-1 chimeric viruses (MA/JFH-1.1 and MA/JFH-1.2) acquired the ability to spread rapidly after long-term culture.

As the characteristics of the MA/JFH-1 virus changed in long-term culture, we analyzed the possible mutations in the viral genome from the supernatant at each peak in core protein levels (Table 1, days at peak core levels). Nine- to 12-nucleotide mutations were found in the viral genome from each supernatant, and the detected mutations were distributed along the entire genome. Among these mutations, a common nonsynonymous mutation was found in the core region (Arg to Gly at amino acid [aa]167, R167G).

In order to test the effects of R167G on virus production, an R167G substitution was introduced into MA/JFH-1.2 as MA/JFH-1.2 replicated and produced infectious virus more efficiently than MA/JFH-1.1. HCV core protein levels in cells and medium of MA/JFH-1.2 with R167G (MA/JFH-1.2/R167G) were higher than with MA/JFH-1.2 ($P < 0.05$) (Fig. 3A and B). HCV RNA levels in the medium of MA/JFH-1.2/R167G RNA-transfected cells were also higher than with MA/JFH-1.2 ($P < 0.05$) (Fig. 3C). Infectious virus production was also increased by the R167G mutation ($P < 0.05$) (Fig. 3D) and was 8.7-fold higher than that of JFH-1 RNA-transfected cells on day 3 ($P < 0.05$) (Fig. 3D).

We then tested whether R167G was responsible for the rapid spread observed in culture supernatant after long-term culture by monitoring virus spread after infection of naïve Huh7.5.1 with culture medium taken 3 days after RNA transfection of MA/JFH-1.2 and MA/JFH-1.2/R167G at an MOI of 0.005. Core protein levels in medium from MA/JFH-1.2/R167G-infected cells increased with the same kinetics as levels of JFH-1 (Fig. 3E), and the population of core protein-positive cells was almost the same as with JFH-1-infected cells (Fig. 3F), indicating that MA/JFH-1.2/R167G virus spread as rapidly as JFH-1 virus. In contrast, we observed no infectious foci in the MA/JFH-1.2 virus-inoculated cells (Fig. 3F). These data suggest that the R167G mutation in the core region was a cell culture-adaptive mutation and that it enhanced infectious MA/JFH-1.2 virus production.

In order to determine whether R167G enhances RNA replication or other steps in the viral life cycle, we performed a single-cycle virus production assay (11) using Huh7-25 cells, a HuH-7-derived cell line lacking CD81 expression on the cell surface (1).

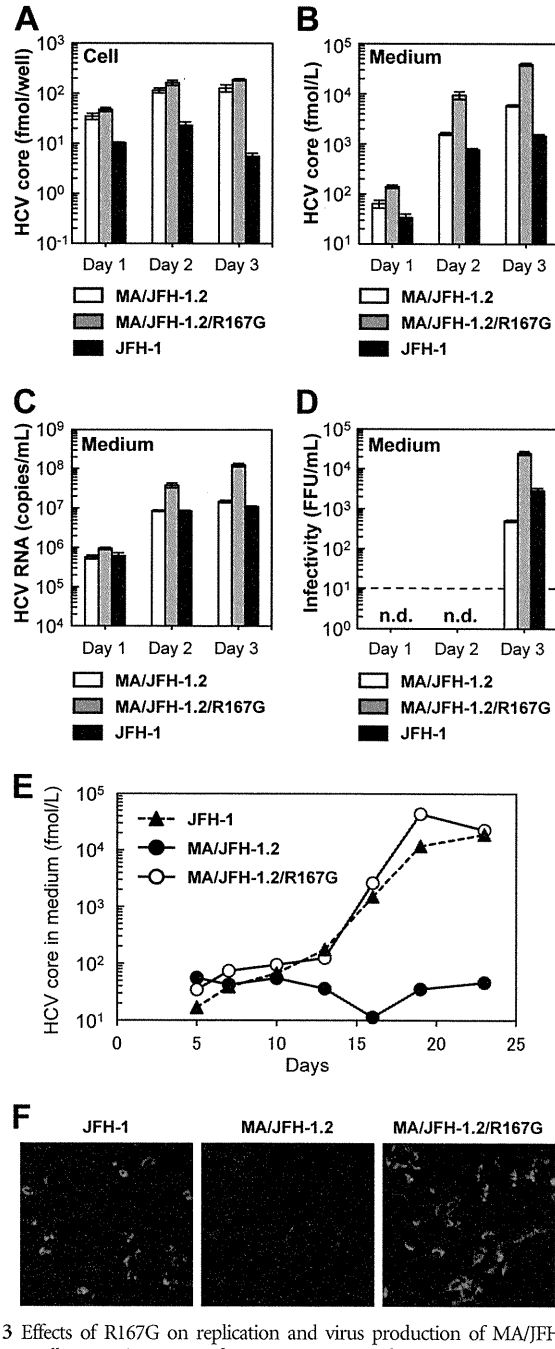

FIG 3 Effects of R167G on replication and virus production of MA/JFH-1.2 in Huh7.5.1 cells. Ten micrograms of HCV RNA was transfected into Huh7.5.1 cells, and cells and medium were harvested on days 1, 2, and 3. HCV core protein levels in the cells (A) and culture medium (B) and HCV RNA levels in the medium (C) and the infectivity of culture medium (D) from HCV RNA-transfected Huh7.5.1 cells are shown. n.d., not determined. Dashed line indicates the detection limit. Assays were performed three times independently, and data are presented as means ± standard deviation. (E) HCV core protein levels in culture medium from cells infected with medium at 3 days posttransfection at an MOI of 0.005. (F) Immunostained cells at 19 days postinfection. Infected cells were visualized with anti-core antibody (green), and nuclei were visualized with DAPI (blue).

This cell line can support replication and infectious virus production upon transfection of HCV genomic RNA but cannot be reinfected by progeny virus, thereby allowing observation of a single cycle of infectious virus production without the confounding ef-

fects of reinfection. R167G did not affect HCV core protein levels in the chimeric RNA-transfected Huh7-25 cells (Fig. 4A), demonstrating that R167G did not enhance RNA replication. Nevertheless, R167G increased HCV core protein levels in the medium ($P < 0.05$ on days 2 and 3) and infectivity (Fig. 4B and C). These results suggest that R167G did not affect RNA replication but affected other steps such as virus assembly and/or virus secretion.

Virus particle assembly efficiency was then assessed by determining intracellular-specific infectivity from infectivity and RNA titer in the cells, as reported previously (11). As shown in Fig. 4G, R167G enhanced intracellular-specific infectivity of MA/JFH-1.2 virus 10.2-fold. Virus secretion efficiency was also calculated from the amount of intracellular and extracellular infectious virus, but R167G had no effect (Fig. 4G).

To confirm the effects of Arg167 in other HCV strains, we tested its effects on JFH-1. As aa 167 of JFH-1 is Gly, we replaced it with Arg (G167R). HCV core protein levels in the cells were not affected by G167R (Fig. 4D), and no effects on RNA replication were confirmed. HCV core protein levels in the medium and infectivity decreased after G167R mutation (Fig. 4E and F). As the G167R mutation decreased intracellular infectious virus production of JFH-1 to undetectable levels, we were unable to determine the intracellular-specific infectivity and virus secretion efficiency of JFH-1 G167R (Fig. 4G). These results indicate that Gly is favored over Arg at core position 167 for infectious virus assembly in multiple HCV strains.

MA harboring the R167G mutation, 5′ UTR, and N3H (NS3 helicase) and N5BX (NS5B to 3′ X) regions of JFH-1 replicated and produced infectious chimeric virus. In order to establish a genotype 2b cell culture system with the MA strain with minimal regions of JFH-1, we attempted to reduce JFH-1 content in MA/JFH-1.2. We previously reported that replacement of the N3H and N5BX regions of JFH-1 allowed efficient replication of the J6CF strain, which normally cannot replicate in cells (21). Thus, we tested whether the N3H and N5BX regions of JFH-1 could also support MA RNA replication.

We prepared two chimeric MA constructs harboring the 5′ UTR and N3H and N5BX regions of JFH-1, MA/N3H+N5BX-JFH1 (Fig. 5A) and MA/N3H+N5BX-JFH1/R167G. After *in vitro* transcribed RNA was transfected into Huh7.5.1 cells, intracellular core protein levels of MA/N3H+N5BX-JFH1 and MA/N3H+N5BX-JFH1/R167G RNA-transfected cells increased in a time-dependent manner and reached almost the same levels as with MA/JFH-1.2 RNA-transfected cells on day 5 (Fig. 5B). Extracellular core protein and HCV RNA levels of MA/N3H+N5BX-JFH1 and MA/N3H+N5BX-JFH1/R167G RNA-transfected cells also increased in a time-dependent manner (Fig. 5C and D). However, they were more than 10 times lower than with MA/JFH-1.2 RNA-transfected cells although intracellular core levels were comparable on day 5 (Fig. 5B to D).

We then tested whether the medium from MA/N3H+N5BX-JFH1 and MA/N3H+N5BX-JFH1/R167G RNA-transfected cells was infectious. Infectivity of the medium from MA/N3H+N5BX-JFH1 RNA-transfected cells was below the detection limit, and that of MA/N3H+N5BX-JFH1/R167G RNA-transfected cells on day 5 was very low ($3.3 \times 10^1 \pm 2.1 \times 10^1$ FFU/ml) (Fig. 5E). To confirm infectivity, the culture media were concentrated, and their infectivity was determined. Infected foci were observed after infection with concentrated medium in MA/N3H+N5BX-JFH1/R167G RNA-transfected cells (Fig. 5F), and infectivity was found

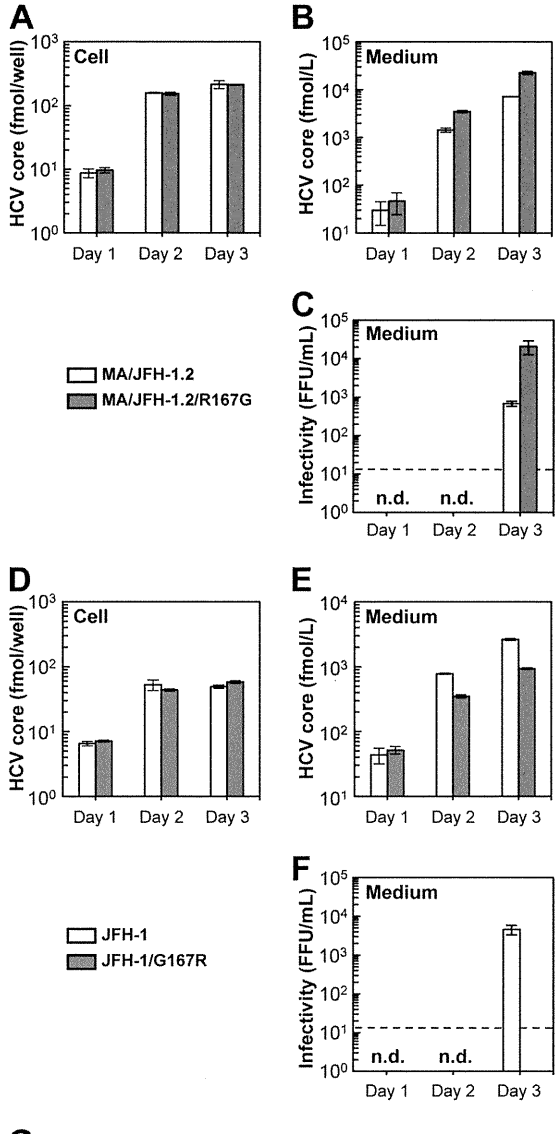

G

Construct	Intracellular Specific Infectivity (FFU/ x10⁶ HCV RNA copies)	Infectious Virus Secretion (Extra/Intra)
MA/JFH-1.2	1.68 ± 0.404	20.2 ± 4.26
MA/JFH-1.2/R167G	17.1 ± 4.38	14.1 ± 1.65
JFH-1	1.78 ± 0.364	63.3 ± 6.44
JFH-1/G167R	NA	NA

FIG 4 Effects of R167G on replication and virus production of MA/JFH-1.2 and JFH-1 in Huh7-25 cells. Ten micrograms of HCV RNA was transfected into Huh7-25 cells, and cells and medium were harvested on days 1, 2, and 3. HCV core protein levels in cells (A and D) and in medium (B and E) were measured, and infectivity of medium (C and F) was determined. n.d., not determined. Dashed line indicates the detection limit. (G) Intracellular specific infectivity and virus secretion efficiency of chimeric HCV RNA-transfected cells. Intracellular and extracellular infectivity of day 3 samples was determined, and specific infectivity and virus secretion rate were calculated. Assays were performed three times independently, and data are presented as means ± standard deviation. NA, not available.

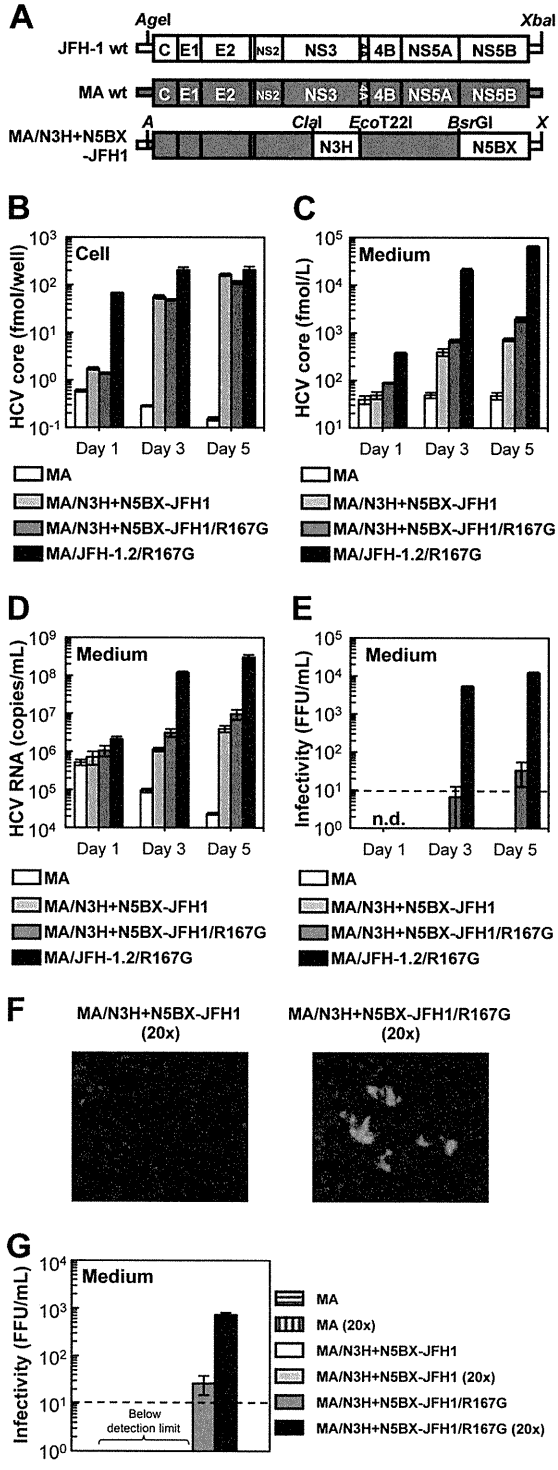

FIG 5 Replication and virus production of MA/N3H+N5BX-JFH1/R167G in Huh7.5.1 cells. (A) Schematic structures of JFH-1, MA, and MA/N3H+N5BX-JFH1. The junction of JFH-1 and MA in the 5′ UTR is an AgeI site; the junctions of MA and JFH-1 in the NS3 regions are ClaI and EcoT22I sites, and the junction in the NS5B region is a BsrGI site. A, AgeI; X, XbaI. (B to G) Chimeric HCV RNA replication in Huh7.5.1 cells. Ten micrograms of HCV RNA was transfected into Huh7.5.1 cells, and cells and medium were harvested on days 1, 3, and 5. HCV core protein levels in cells (B) and in medium (C) and HCV RNA levels in medium (D) were measured, and infectivity of medium (E) was determined. Assays were performed three times independently, and data are presented as means ± standard deviation. n.d., not determined. Dashed line indicates the detection limit. (F) Immunostained cells. Huh7.5.1 cells were infected with concentrated medium from RNA-transfected cells on day 5. Infected cells were visualized with anti-core antibody (green), and nuclei were visualized with DAPI (blue). (G) Infectivity of concentrated culture medium from HCV RNA-transfected cells. Culture medium was concentrated by 20 times. Infectivities of original and concentrated culture media were determined. Dashed line indicates detection thelimit.

to be $7.27 \times 10^2 \pm 7.57 \times 10^1$ FFU/ml (Fig. 5G). No infected foci were observed after infection of MA/N3H+N5BX-JFH1 RNA-transfected cells, even when medium was concentrated (Fig. 5F), although intracellular and extracellular core protein levels were comparable to those with MA/N3H+N5BX-JFH1/R167G RNA-transfected cells (Fig. 5B and C). These results indicate that replacement of the 5′ UTR and N3H and N5BX regions in JFH-1 were necessary to rescue autonomous replication in the replication-incompetent MA strain and for secretion of infectious chimeric virus. However, the secretion and infection efficiencies of the virus were low.

Cell culture-adaptive mutations enhanced infectious virus production of MA/N3H+N5BX-JFH1/R167G. Because MA/N3H+N5BX-JFH1/R167G replicated efficiently but produced very small amounts of infectious virus, we performed a long-term culture of the RNA-transfected cells in order to induce cell culture-adaptive mutations that could enhance infectious virus production. We prepared RNA-transfected cells using two constructs, MA/N3H+N5BX-JFH1 and MA/N3H+N5BX-JFH1/R167G; both of these replicated efficiently, and MA/N3H+N5BX-JFH1/R167G produced infectious virus at low levels while MA/N3H+N5BX-JFH1 did not. Immediately after transfection, the HCV core protein levels in the medium of each RNA-transfected cell culture peaked at 3.0×10^3 fmol/liter and declined thereafter. However, the core protein level in the medium with MA/N3H+N5BX-JFH1/R167G RNA-transfected cells continued to increase and reached a peak of 2.7×10^5 fmol/liter 54 days after transfection, at which point most cells were core protein positive (Fig. 6B). The core protein level in the medium with MA/N3H+N5BX-JFH1 RNA-transfected cells did not increase and core-positive cells were scarce on day 54 (Fig. 6B). We analyzed the viral genome in the culture supernatants from day 54 for possible mutations and identified four nonsynonymous mutations in the MA/N3H+N5BX-JFH1/R167G genome: L814S (NS2), R1012G, (NS2), T1106A (NS3), and V1951A (NS4B). In order to test whether these amino acid substitutions enhance infectious virus production, L814S, R1012G, T1106A, and V1951A were introduced into MA/N3H+N5BX-JFH1/R167G, and the product was designated MA/N3H+N5BX-JFH1/5am (where am indicates adaptive mutation). On day 1, although HCV core protein levels in the MA/N3H+N5BX-JFH1/5am RNA-transfected cells were higher than those of MA/N3H+N5BX-JFH1/R167G RNA-transfected cells, they were still lower than those of MA/JFH-1.2/R167G RNA-transfected cells; however, on days 3 and 5, they reached a level comparable to that of MA/JFH-1.2/R167G RNA-transfected cells (Fig. 6C). HCV core protein and HCV RNA levels in the medium of MA/N3H+N5BX-JFH1/5am RNA-transfected cells were higher than those of MA/JFH-1.2/R167G RNA-transfected cells ($P < 0.05$, Fig. 6D and 6E, respectively). MA/N3H+N5BX-JFH1/5am, containing the four additional adaptive mutations, produced infectious virus at the same level as MA/JFH-1.2/R167G on day 5 (Fig. 6F). These results indicate that the

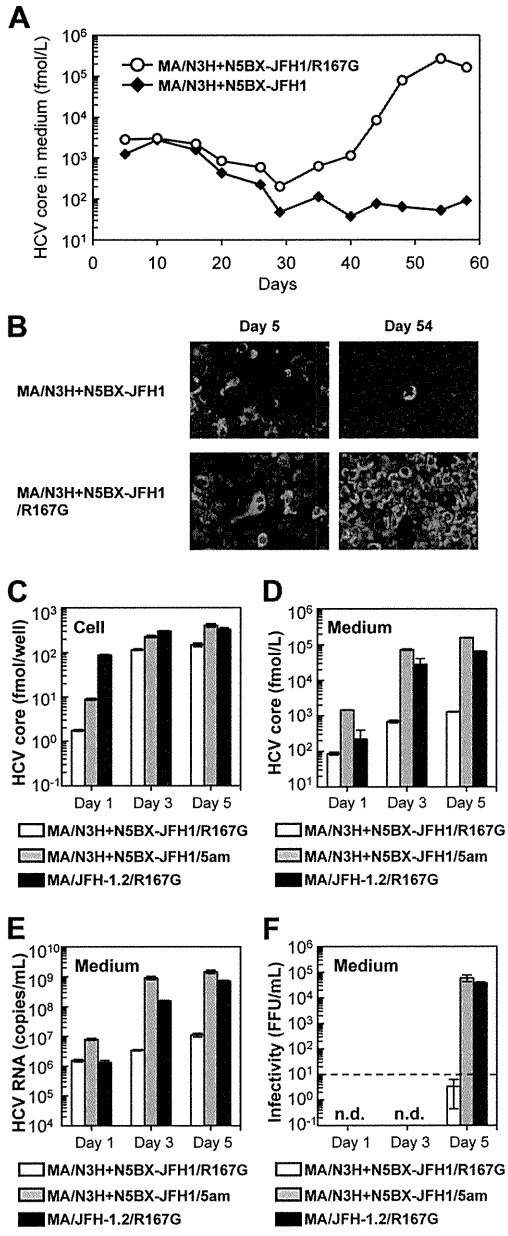

FIG 6 Cell culture-adaptive mutations enhanced infectious virus production of MA/N3H+N5BX-JFH1/R167G. (A) Long-term culture of MA/N3H+N5BX-JFH1 and MA/N3H+N5BX-JFH1/R167G RNA-transfected cells. Ten micrograms of HCV RNA was transfected into Huh7.5.1 cells, and cells were passaged every 2 to 5 days, depending on cell status. Culture medium was collected after every passage, and HCV core protein levels were measured. HCV core protein levels in culture medium from MA/N3H+N5BX-JFH1 and MA/N3H+N5BX-JFH1/R167G RNA-transfected cells are presented. (B) Immunostained cells on days 5 and 54 after transfection. Infected cells were visualized with anti-core antibody (green), and nuclei were visualized with DAPI (blue). (C to F) Effect of four additional cell culture-adaptive mutations on virus production. Ten micrograms of HCV RNA was transfected into Huh7.5.1 cells, and cells and medium were harvested on days 1, 3, and 5. HCV core levels in cells (C) and in medium (D) and HCV RNA levels in medium (E) were measured, and infectivity of medium (F) was determined. Assays were performed three times independently, and data are presented as means ± standard deviation. n.d., not determined. Dashed line indicates the detection limit.

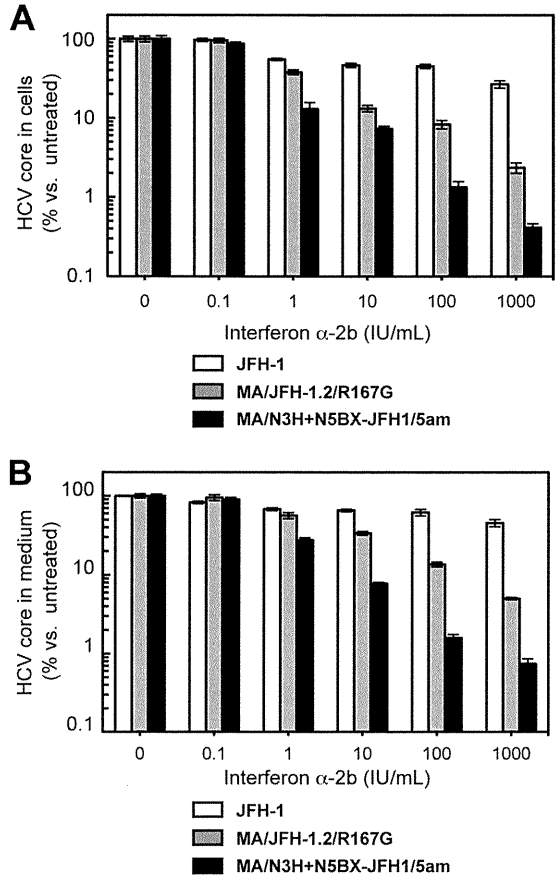

FIG 7 Comparisons of interferon sensitivity between JFH-1, MA/JFH-1.2/R167G and MA/N3H+N5BX-JFH1/5am. Two micrograms of HCV RNA was transfected into Huh7.5.1 cells, and interferon was added at the indicated concentrations at 4 h after transfection. HCV core protein levels in cells (A) and in medium (B) on day 3 were measured, and data are expressed as percent versus untreated cells (0 IU/ml). Assays were performed three times independently, and data are presented as means ± standard deviation.

four additional adaptive mutations enhance infectious virus production and that MA/N3H+N5BX-JFH1/5am RNA-transfected cells replicate and produce infectious virus as efficiently as MA/JFH-1.2/R167G RNA-transfected cells.

Comparison of interferon sensitivity between JFH-1, MA/JFH-1.2/R167G, and MA/N3H+N5BX-JFH1/R167G. Using the newly established genotype 2b infectious chimeric virus, we compared interferon sensitivity between the JFH-1, MA/JFH-1.2/R167G, and MA/N3H+N5BX-JFH1/5am viruses. JFH-1 or MA chimeric viral RNA-transfected Huh7.5.1 cells were treated with 0.1, 1, 10, 100, or 1,000 IU/ml interferon α-2b, and HCV core protein levels in the cells and in culture media were compared. Interferon decreased HCV core protein levels in the JFH-1 RNA-transfected cells and in the medium in a dose-dependent manner, and production was inhibited to 26.8% ± 3.0% and 45.6% ± 4.7%, respectively, of control levels (Fig. 7A and B, respectively). In contrast, HCV core protein levels in cells and medium of MA/JFH-1.2/R167G and MA/N3H+N5BX-JFH1/5am RNA-transfected cells decreased more pronouncedly in a dose-dependent manner (Fig. 7A and B, respectively). HCV core protein levels in cells and medium from MA/N3H+N5BX-JFH1/5am RNA-transfected cells were lower than those from MA/JFH-1.2/

R167G RNA-transfected cells (Fig. 7A and B, respectively) ($P < 0.05$ at 1, 10, 100, and 1,000 IU/ml), indicating that the MA/N3H+N5BX-JFH1/5am virus was more sensitive to interferon than the MA/JFH1.2/R167G virus, which contained more regions from JFH-1.

DISCUSSION

In this study, we developed a novel infectious HCV production system using a genotype 2b chimeric virus. To improve infectious virus production, we introduced two modifications into the chimeric genome.

First, we replaced the 5′ UTR from MA with that of JFH-1. Similarly to J6/JFH-1, replacement of the 5′ UTR increased core protein accumulation in both the cells and medium when these RNAs were transfected into Huh7.5.1 cells (Fig. 1). The same trend was observed when these RNAs were transfected into Huh7-25 cells (data not shown), indicating that the 5′ UTR of JFH-1 enhanced RNA replication. There are two genetic variations in J6CF and seven in MA in the region we replaced (nt 1 to 154 for J6CF and nt 1 to 155 for MA), and some of these mutations may affect RNA replication by changing the RNA secondary structure, RNA-RNA interactions, or binding of host or viral proteins.

Second, we introduced a cell culture-adaptive mutation (R167G) in the core region. This mutation was induced by long-term culture of MA/JFH-1 RNA-transfected cells (Fig. 2). MA/JFH-1 chimeric RNA (MA/JFH-1.1 and MA/JFH-1.2) replicated when synthesized RNA was transfected into the cells. However, infectious virus production was low, and virus infection did not spread over the short term. In early stages of long-term culture, the number of core protein-positive cells gradually decreased, and core protein-positive cells were scarcely detectable. Subsequently, the population of core protein-positive cells increased, reaching almost 100%. At this time point, we identified a common mutation in the core region (R167G) of the viral genome as a cell culture-adaptive mutation and found that it enhanced infectious virus production (Fig. 3). Several nonsynonymous mutations other than R167G were identified in the viral genome from each supernatant, and these mutations may enhance infectious virus production. However, there was a discrepancy between RNA levels and the infectivity of the culture media of MA/JFH-1.2 and MA/JFH-1.2/R167G RNA-transfected cells (Fig. 3C and D). The MA/JFH-1.2/R167G mutant had a 2-log increase in viral infectivity compared to that of MA/JFH-1.2 but only a 1-log increase in secreted RNA. The replication efficiency of MA/JFH-1.2 RNA-transfected cells was comparable to that of MA/JFH-1.2/R167G RNA-transfected cells, but the efficiency of infectious virus assembly within the cells was low, indicating that mainly noninfectious virus may be produced.

Infection of MA/JFH-1.2/R167G virus spreads rapidly, similarly to that of the JFH-1 virus, when it is inoculated into naïve Huh7.5.1 cells. On a single-cycle virus production assay, we found that the R167G mutation did not affect RNA replication or virus secretion but enhanced infectious virus assembly within the cells (Fig. 4). Efficient infectious virus assembly within the cells was mainly responsible for the rapid spread and high virus production of MA/JFH-1.2/R167G.

The amino acid at 167 (aa 167) is located in domain 2 of the core region, which is important for localization of the core protein (3, 8). Lipid droplet localization of the core protein and/or NS5A is important for infectious virus production (4, 18, 26). The interaction between the core protein and NS5A is also important for infectious virus production (16). Thus, aa 167 affects infectious virus production possibly by altering subcellular localization of the core protein or interaction between the core protein and NS5A. We examined the amino acid sequence of the core protein in 2,078 strains in the Hepatitis Virus Database (http://s2as02.genes.nig.ac.jp/) and found that aa 167 is Gly in all other strains. These data strongly suggest that Gly at aa 167 is important for the HCV life cycle. As the MA strain was cloned from the serum of a patient with chronic hepatitis C, the low virus production by this Gly at aa 167 may be important for persistent infection.

We then attempted to reduce the contents of JFH-1 from MA/JFH-1.2/R167G. We previously reported that the N3H and N5BX regions of JFH-1 were sufficient for replication of the J6CF strain (21). We also reported that this effect was observed only in genotype 2a strains (J6CF, JCH-1, and JCH-4). In this study, we tested whether the N3H and N5BX regions of JFH-1 could also support replication of a genotype 2b strain, MA. We constructed an MA chimeric virus harboring the N3H and N5BX regions of JFH-1 and combined this with the 5′ UTR of JFH-1 and the R167G mutation (MA/N3H+N5BX-JFH1/R167G). This chimeric RNA was able to replicate in the cells and produce infectious chimeric virus in culture medium although infectious virus production levels were low (Fig. 5).

We showed in this paper that the N3H and N5BX regions of JFH-1 were able to support RNA replication by both genotype 2a clones and genotype 2b clones, but the nucleotide sequence similarity between JFH-1 and MA was lower than that between JFH-1 and J6CF (77% versus 89%, respectively). Compared to MA/JFH-1.2/R167G, MA/N3H+N5BX-JFH1/R167G RNA showed the same levels of RNA replication and low levels of infectious virus production. To clarify whether there were any differences in the characteristics of the secreted virus, we performed density gradient ultracentrifugation with the MA/JFH-1.2/R167G and MA/N3H+N5BX-JFH1/R167G viruses. The distributions of the HCV core protein and infectivity showed similar profiles (data not shown).

The differences between MA/JFH-1.2/R167G and MA/N3H+N5BX-JFH1/R167G are the NS2, NS3 protease domain (N3P), and NS4A to NS5A regions. Nucleotide variation(s) other than aa 167 in these regions of the MA strain may be associated with reduced virus assembly. We identified four additional cell culture-adaptive mutations, L814S (NS2), R1012G (NS2), T1106A (NS3), and V1951A (NS4B), which resulted from long-term culture of MA/N3H+N5BX-JFH1/R167G RNA-transfected cells. Consequently, cells transfected with MA/N3H+N5BX-JFH1/5am constructed by insertion of these four adaptive mutations into MA/N3H+N5BX-JFH1/R167G replicated and produced infectious virus as efficiently as MA/JFH-1.2/R167G RNA-transfected cells (Fig. 6).

This system is able to contribute to studies into the development of antiviral strategies. It has been reported that HCV genotype 2a was more sensitive to interferon therapy than HCV genotype 2b in a clinical study (20). To assess the interferon resistance of genotype 2b, a cell culture system with multiple genotype 2b strains is necessary. The previously reported replicable genotype 2b chimeric virus harbored only structural

regions of 2b strains (6, 27). The 2b/JFH-1 chimeric virus containing the region of the core protein to NS2 from the J8 strain (genotype 2b) and the region of NS3 to 3′ X of JFH-1 was able to replicate and showed that there were no differences in interferon sensitivity among the JFH-1 chimeric viruses of other genotypes (6, 27). Another 2b/JFH-1 chimeric virus containing the regions of the core protein to NS2 (nt 342 to 2867) of a genotype 2b strain and of NS2 to 3′ UTR (nt 2868) of JFH-1 has been reported (6, 27). The authors reported that their 2b/JFH-1 chimeric virus was more sensitive to interferon than JFH-1 (6, 27). We developed the genotype 2b HCV cell culture system with another HCV genotype 2b strain (MA). We identified a virus assembly-enhancing mutation in the core region, the minimal JFH-1 regions necessary for replication, and four additional adaptive mutations that enhance infectious virus production and demonstrated that MA harboring the five adaptive mutations and the 5′ UTR and N3H and N5BX regions of JFH-1 (MA/N3H+N5BX-JFH1/5am) could replicate and produce infectious virus efficiently.

Using these novel genotype 2b chimeric viruses, we assessed interferon sensitivity. We found that MA/JFH-1.2/R167G chimeric virus and MA/N3H+N5BX-JFH1/5am virus were more sensitive to interferon than the JFH-1 virus (Fig. 7). Furthermore, we found that MA/N3H+N5BX-JFH1/5am was more sensitive to interferon than MA/JFH-1.2/R167G, indicating that the genetic variation(s) in the NS2, N3P, and NS4A to NS5A regions affect interferon sensitivity. Although genotype 2a viruses are more sensitive to interferon than genotype 2b viruses in clinical studies, JFH-1 displayed interferon resistance in our study.

These results suggest that the JFH-1 regions in the 2b/JFH-1 virus affect the interferon sensitivity of the chimeric virus. Moreover, it was reported that amino acid variations in E2, p7, NS2, and NS5A were associated with the response to peginterferon and ribavirin therapy in genotype 2b HCV infection (10). Therefore, our MA/JFH-1 chimeric virus harboring minimal regions from JFH-1 (MA/N3H+N5BX-JFH1/5am) is more suitable for assessing the characteristics of the MA strain than the MA/JFH-1 chimeric virus, which includes a nonstructural region from JFH-1 (MA/JFH-1.2/R167G). We showed here that replacement of the 5′ UTR and N3H and N5BX regions in MA with those from JFH-1 is able to convert MA into a replicable virus. Using the same strategy, numerous HCV cell culture systems with various genotype 2b strains, as well as genotype 2a strains, may be available.

In conclusion, we established a novel HCV genotype 2b cell culture system using a chimeric genome in MA harboring minimal regions from JFH-1. This cell culture system using the chimeric genotype 2b virus will be useful for characterization of genotype 2b viruses and the development of antiviral strategies.

ACKNOWLEDGMENTS

We are grateful to Tetsuro Suzuki of Hamamatsu University School of Medicine for helpful comments and suggestions. Huh7.5.1 cells were kindly provided by Francis V. Chisari.

A.M. is partially supported by the Japan Health Sciences Foundation and Viral Hepatitis Research Foundation of Japan. This work was partially supported by Grants-in-Aid for Scientific Research from the Japan Society for the Promotion of Science, from the Ministry of Health, Labor and Welfare of Japan, from the Ministry of Education, Culture, Sports, Science and Technology, from the National Institute of Biomedical Innovation, and by Research on Health Sciences Focusing on Drug Innovation from the Japan Health Sciences Foundation.

REFERENCES

1. **Akazawa D, et al.** 2007. CD81 expression is important for the permissiveness of Huh7 cell clones for heterogeneous hepatitis C virus infection. J. Virol. **81**:5036–5045.
2. **Bartenschlager R, Lohmann V.** 2000. Replication of hepatitis C virus. J. Gen. Virol. **81**:1631–1648.
3. **Boulant S, et al.** 2006. Structural determinants that target the hepatitis C virus core protein to lipid droplets. J. Biol. Chem. **281**:22236–22247.
4. **Boulant S, Targett-Adams P, McLauchlan J.** 2007. Disrupting the association of hepatitis C virus core protein with lipid droplets correlates with a loss in production of infectious virus. J. Gen. Virol. **88**:2204–2213.
5. **Choo QL, et al.** 1989. Isolation of a cDNA clone derived from a blood-borne non-A, non-B viral hepatitis genome. Science **244**:359–362.
6. **Gottwein JM, et al.** 2009. Development and characterization of hepatitis C virus genotype 1–7 cell culture systems: role of CD81 and scavenger receptor class B type I and effect of antiviral drugs. Hepatology **49**:364–377.
7. **Griffin S, et al.** 2008. Genotype-dependent sensitivity of hepatitis C virus to inhibitors of the p7 ion channel. Hepatology **48**:1779–1790.
8. **Hope RG, McLauchlan J.** 2000. Sequence motifs required for lipid droplet association and protein stability are unique to the hepatitis C virus core protein. J. Gen. Virol. **81**:1913–1925.
9. **Jensen TB, et al.** 2008. Highly efficient JFH1-based cell-culture system for hepatitis C virus genotype 5a: failure of homologous neutralizing-antibody treatment to control infection. J. Infect. Dis. **198**:1756–1765.
10. **Kadokura M, et al.** 2011. Analysis of the complete open reading frame of genotype 2b hepatitis C virus in association with the response to peginterferon and ribavirin therapy. PLoS One **6**:e24514.
11. **Kato T, et al.** 2008. Hepatitis C virus JFH-1 strain infection in chimpanzees is associated with low pathogenicity and emergence of an adaptive mutation. Hepatology **48**:732–740.
12. **Kato T, et al.** 2006. Cell culture and infection system for hepatitis C virus. Nat. Protoc. **1**:2334–2339.
13. **Kiyosawa K, et al.** 1990. Interrelationship of blood transfusion, non-A, non-B hepatitis and hepatocellular carcinoma: analysis by detection of antibody to hepatitis C virus. Hepatology **12**:671–675.
14. **Lindenbach BD, et al.** 2005. Complete replication of hepatitis C virus in cell culture. Science **309**:623–626.
15. **Lohmann V, et al.** 1999. Replication of subgenomic hepatitis C virus RNAs in a hepatoma cell line. Science **285**:110–113.
16. **Masaki T, et al.** 2008. Interaction of hepatitis C virus nonstructural protein 5A with core protein is critical for the production of infectious virus particles. J. Virol. **82**:7964–7976.
17. **Miyamoto M, Kato T, Date T, Mizokami M, Wakita T.** 2006. Comparison between subgenomic replicons of hepatitis C virus genotypes 2a (JFH-1) and 1b (Con1 NK5.1). Intervirology **49**:37–43.
18. **Miyanari Y, et al.** 2007. The lipid droplet is an important organelle for hepatitis C virus production. Nat. Cell Biol. **9**:1089–1097.
19. **Murakami K, Abe M, Kageyama T, Kamoshita N, Nomoto A.** 2001. Down-regulation of translation driven by hepatitis C virus internal ribosomal entry site by the 3′ untranslated region of RNA. Arch. Virol. **146**:729–741.
20. **Murakami T, et al.** 1999. Mutations in nonstructural protein 5A gene and response to interferon in hepatitis C virus genotype 2 infection. Hepatology **30**:1045–1053.
21. **Murayama A, et al.** 2007. The NS3 helicase and NS5B-to-3′X regions are important for efficient hepatitis C virus strain JFH-1 replication in Huh7 cells. J. Virol. **81**:8030–8040.
22. **Murayama A, et al.** 2010. RNA polymerase activity and specific RNA structure are required for efficient HCV replication in cultured cells. PLoS Pathog. **6**:e1000885.
23. **Pietschmann T, et al.** 2006. Construction and characterization of infectious intragenotypic and intergenotypic hepatitis C virus chimeras. Proc. Natl. Acad. Sci. U. S. A. **103**:7408–7413.
24. **Pietschmann T, et al.** 2009. Production of infectious genotype 1b virus particles in cell culture and impairment by replication enhancing mutations. PLoS Pathog. **5**:e1000475.
25. **Scheel TK, et al.** 2008. Development of JFH1-based cell culture systems

for hepatitis C virus genotype 4a and evidence for cross-genotype neutralization. Proc. Natl. Acad. Sci. U. S. A. **105**:997–1002.
26. **Shavinskaya A, Boulant S, Penin F, McLauchlan J, Bartenschlager R.** 2007. The lipid droplet binding domain of hepatitis C virus core protein is a major determinant for efficient virus assembly. J. Biol. Chem. **282**: 37158–37169.
27. **Suda G, et al.** 2010. IL-6-mediated intersubgenotypic variation of interferon sensitivity in hepatitis C virus genotype 2a/2b chimeric clones. Virology **407**:80–90.
28. **Takeuchi T, et al.** 1999. Real-time detection system for quantification of hepatitis C virus genome. Gastroenterology **116**:636–642.
29. **Wakita T, et al.** 2005. Production of infectious hepatitis C virus in tissue culture from a cloned viral genome. Nat. Med. **11**:791–796.
30. **Yi M, Ma Y, Yates J, Lemon SM.** 2007. Compensatory mutations in E1, p7, NS2, and NS3 enhance yields of cell culture-infectious intergenotypic chimeric hepatitis C virus. J. Virol. **81**:629–638.
31. **Yi M, Villanueva RA, Thomas DL, Wakita T, Lemon SM.** 2006. Production of infectious genotype 1a hepatitis C virus (Hutchinson strain) in cultured human hepatoma cells. Proc. Natl. Acad. Sci. U. S. A. **103**:2310–2315.
32. **Zhong J, et al.** 2005. Robust hepatitis C virus infection in vitro. Proc. Natl. Acad. Sci. U. S. A. **102**:9294–9299.

Efficient Generation of Functional Hepatocytes From Human Embryonic Stem Cells and Induced Pluripotent Stem Cells by HNF4α Transduction

Kazuo Takayama[1,2], Mitsuru Inamura[1,2], Kenji Kawabata[2,3], Kazufumi Katayama[1], Maiko Higuchi[2], Katsuhisa Tashiro[2], Aki Nonaka[2], Fuminori Sakurai[1], Takao Hayakawa[4,5], Miho Kusuda Furue[6,7] and Hiroyuki Mizuguchi[1,2,8]

[1]Laboratory of Biochemistry and Molecular Biology, Graduate School of Pharmaceutical Sciences, Osaka University, Osaka, Japan; [2]Laboratory of Stem Cell Regulation, National Institute of Biomedical Innovation, Osaka, Japan; [3]Laboratory of Biomedical Innovation, Graduate School of Pharmaceutical Sciences, Osaka University, Osaka, Japan; [4]Pharmaceutics and Medical Devices Agency, Tokyo, Japan; [5]Pharmaceutical Research and Technology Institute, Kinki University, Osaka, Japan; [6]JCRB Cell Bank, Division of Bioresources, National Institute of Biomedical Innovation, Osaka, Japan; [7]Laboratory of Cell Processing, Institute for Frontier Medical Sciences, Kyoto University, Kyoto, Japan; [8]The Center for Advanced Medical Engineering and Informatics, Osaka University, Osaka, Japan

Hepatocyte-like cells from human embryonic stem cells (ESCs) and induced pluripotent stem cells (iPSCs) are expected to be a useful source of cells drug discovery. Although we recently reported that hepatic commitment is promoted by transduction of SOX17 and HEX into human ESC- and iPSC-derived cells, these hepatocyte-like cells were not sufficiently mature for drug screening. To promote hepatic maturation, we utilized transduction of the hepatocyte nuclear factor 4α (HNF4α) gene, which is known as a master regulator of liver-specific gene expression. Adenovirus vector-mediated overexpression of HNF4α in hepatoblasts induced by SOX17 and HEX transduction led to upregulation of epithelial and mature hepatic markers such as cytochrome P450 (CYP) enzymes, and promoted hepatic maturation by activating the mesenchymal-to-epithelial transition (MET). Thus HNF4α might play an important role in the hepatic differentiation from human ESC-derived hepatoblasts by activating the MET. Furthermore, the hepatocyte like-cells could catalyze the toxication of several compounds. Our method would be a valuable tool for the efficient generation of functional hepatocytes derived from human ESCs and iPSCs, and the hepatocyte-like cells could be used for predicting drug toxicity.

Received 19 July 2011; accepted 28 September 2011; published online 8 November 2011. doi:10.1038/mt.2011.234

INTRODUCTION

Human embryonic stem cells (ESCs) and induced pluripotent stem cells (iPSCs) are able to replicate indefinitely and differentiate into most of the body's cell types.[1,2] They could provide an unlimited source of cells for various applications. Hepatocyte-like cells, which are differentiated from human ESCs and iPSCs, would be useful for basic research, regenerative medicine, and drug discovery.[3] In particular, it is expected that hepatocyte-like cells will be utilized as a tool for cytotoxicity screening in the early phase of pharmaceutical development. To catalyze the toxication of several compounds, hepatocyte-like cells need to be mature enough to exhibit hepatic functions, including high activity levels of the cytochrome P450 (CYP) enzymes. Because the present technology for the generation of hepatocyte-like cells from human ESCs and iPSCs, which is expected to be utilized for drug discovery, is not refined enough for this application, it is necessary to improve the efficiency of hepatic differentiation. Although conventional methods such as growth factor-mediated hepatic differentiation are useful to recapitulate liver development, they lead to only a heterogeneous hepatocyte population.[4–6] Recently, we showed that transcription factors are transiently transduced to promote hepatic differentiation in addition to the conventional differentiation method which uses only growth factors.[7] Ectopic expression of Sry-related HMG box 17 (SOX17) or hematopoietically expressed homeobox (HEX) by adenovirus (Ad) vectors in human ESC-derived mesendoderm or definitive endoderm (DE) cells markedly enhances the endoderm differentiation or hepatic commitment, respectively.[7,8] However, further hepatic maturation is required for drug screening.

The transcription factor hepatocyte nuclear factor 4α (HNF4α) is initially expressed in the developing hepatic diverticulum on E8.75,[9,10] and its expression is elevated as the liver develops. A previous loss-of-function study showed that HNF4α plays a critical role in liver development; conditional deletion of *HNF4α* in fetal hepatocytes results in the faint expression of many mature hepatic enzymes and the impairment of normal liver morphology.[11] The genome-scale chromatin immunoprecipitation assay showed that HNF4α binds to the promoters of nearly half of the genes expressed in the mouse liver,[12] including cell adhesion and junctional proteins,[13] which are important in

Correspondence: *Hiroyuki Mizuguchi, Laboratory of Biochemistry and Molecular Biology, Graduate School of Pharmaceutical Sciences, Osaka University, 1-6 Yamadaoka, Suita, Osaka 565-0871, Japan. E-mail: mizuguch@phs.osaka-u.ac.jp*

the hepatocyte epithelial structure.[14] In addition, HNF4α plays a critical role in hepatic differentiation and in a wide variety of liver functions, including lipid and glucose metabolism.[15,16] Although HNF4α could promote transdifferentiation into hepatic lineage from hematopoietic cells,[17] the function of HNF4α in hepatic differentiation from human ESCs and iPSCs remains unknown. A previous study showed that hepatic differentiation from mouse hepatic progenitor cells is promoted by HNF4α, although many of the hepatic markers that they examined were target genes of HNF4α.[18] They transplanted the HNF4α-overexpressed mouse hepatic progenitor cells to promote hepatic differentiation, but they did not examine the markers that relate to hepatic maturation such as CYP enzymes, conjugating enzymes, and hepatic transporters.

In this study, we examined the role of HNF4α in hepatic differentiation from human ESCs and iPSCs. The human ESC- and iPSC-derived hepatoblasts, which were efficiently generated by sequential transduction of SOX17 and HEX, were transduced with HNF4α-expressing Ad vector (Ad-HNF4α), and then the expression of hepatic markers of the hepatocyte-like cells were assessed. In addition, we examined whether or not the hepatocyte-like cells, which were generated by sequential transduction of SOX17, HEX, and HNF4α, were able to predict the toxicity of several compounds.

RESULTS

Stage-specific HNF4α transduction in hepatoblasts selectively promotes hepatic differentiation

The transcription factor HNF4α plays an important role in both liver generation[11] and hepatic differentiation from human ESCs and iPSCs (**Supplementary Figure S1**). We expected that hepatic differentiation could be accelerated by HNF4α transduction. To examine the effect of forced expression of HNF4α in the hepatic differentiation from human ESC- and iPSC-derived cells, we used a fiber-modified Ad vector.[19] Initially, we optimized the time period for Ad-HNF4α transduction. Human ESC (H9)-derived DE cells (day 6) (**Supplementary Figures S2** and **S3a**), hepatoblasts (day 9) (**Supplementary Figures S2** and **S3b**), or a heterogeneous population consisting of hepatoblasts, hepatocytes, and cholangiocytes (day 12) (**Supplementary Figures S2** and **S3c**) were transduced with Ad-HNF4α and then the Ad-HNF4α-transduced cells were cultured until day 20 of differentiation (**Figure 1**). We ascertained the expression of exogenous *HNF4α* in human ESC-derived hepatoblasts (day 9) transduced with Ad-HNF4α (**Supplementary Figure S4**). The transduction of Ad-HNF4α into human ESC-derived hepatoblasts (day 9) led to the highest expression levels of the hepatocyte markers *albumin* (*ALB*)[20] and *α-1-antitrypsin* (**Figure 1a**). In contrast, the expression levels of the cholangiocyte markers *cytokeratin 7* (*CK7*)[21] and *SOX9*[22] were

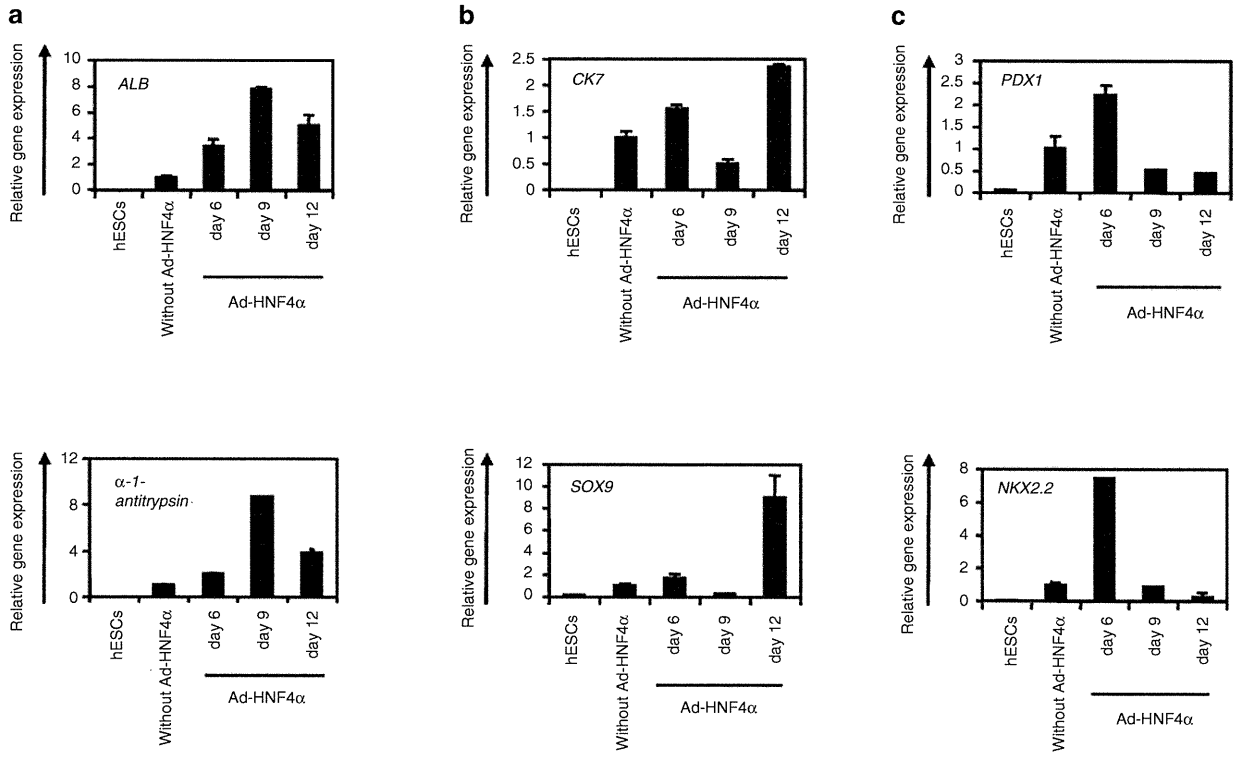

Figure 1 Transduction of HNF4α into hepatoblasts promotes hepatic differentiation. (**a–c**) The human ESC (H9)-derived cells, which were cultured for 6, 9, or 12 days according to the protocol described in **Figure 2a**, were transduced with 3,000 vector particles (VP)/cell of Ad-HNF4α for 1.5 hours and cultured until day 20. The gene expression levels of (**a**) hepatocyte markers (*ALB* and *α-1-antitrypsin*), (**b**) cholangiocyte markers (*CK7* and *SOX9*), and (**c**) pancreas markers (*PDX1* and *NKX2.2*) were examined by real-time RT-PCR on day 0 (human ESCs (hESCs)) or day 20 of differentiation. The horizontal axis represents the days when the cells were transduced with Ad-HNF4α. On the y-axis, the level of the cells without Ad-HNF4α transduction on day 20 was taken as 1.0. All data are represented as means ± SD (n = 3). ESC, embryonic stem cell; HNF4α, hepatocyte nuclear factor 4α; RT-PCR, reverse transcription-PCR.

downregulated in the cells transduced on day 9 as compared with nontransduced cells (**Figure 1b**). This might be because hepatic differentiation was selectively promoted and biliary differentiation was repressed by the transduction of HNF4α in hepatoblasts. The expression levels of the pancreas markers *PDX1*[23] and *NKX2.2*[24] did not make any change in the cells transduced on day 9 as compared with nontransduced cells (**Figure 1c**). Interestingly, the expression levels of the pancreas markers were upregulated, when Ad-HNF4α transduction was performed into DE cells (day 6) (**Figure 1c**). These results suggest that HNF4α might promote not only hepatic differentiation but also pancreatic differentiation, although the optimal stage of HNF4 transduction for the differentiation of each cell is different. We have confirmed that there was no difference between nontransduced cells and Ad-LacZ-transduced cells in the gene expression levels of all the markers investigated in **Figure 1a–c** (data not shown). We also confirmed that Ad vector-mediated gene expression in the human ESC-derived hepatoblasts (day 9) continued until day 14 and almost disappeared on day 18 (**Supplementary Figure S5**). These results indicated that the stage-specific HNF4α overexpression in human ESC-derived hepatoblasts (day 9) was essential for promoting efficient hepatic differentiation.

Transduction of HNF4α into human ESC- and iPSC-derived hepatoblasts efficiently promotes hepatic maturation

From the results of **Figure 1**, we decided to transduce hepatoblasts (day 9) with Ad-HNF4α. To determine whether hepatic maturation is promoted by Ad-HNF4α transduction, Ad-HNF4α-transduced cells were cultured until day 20 of differentiation according to the schematic protocol described in **Figure 2a**. After the hepatic maturation, the morphology of human ESCs was gradually changed into that of hepatocytes: polygonal with distinct round nuclei (day 20) (**Figure 2b**). Interestingly, a portion of the hepatocyte-like cells, which were ALB[20]-, CK18[21]-, CYP2D6-, and CYP3A4[25]-positive cells, had double nuclei, which was also observed in primary human hepatocytes (**Figure 2b,c**, and **Supplementary Figure S6**). We also examined the hepatic gene expression levels on day 20 of differentiation (**Figure 3a,b**). The gene expression analysis of *CYP1A2*, *CYP2C9*, *CYP2C19*, *CYP2D6*, *CYP3A4*, and *CYP7A1*[25] showed higher expression levels in all of Ad-SOX17-, Ad-HEX-, and Ad-HNF4α-transduced cells (three factors-transduced cells) as compared with those in both Ad-SOX17- and Ad-HEX-transduced cells (two factors-transduced cells) on day 20 (**Figure 3a**). The gene expression level of NADPH-CYP reductase

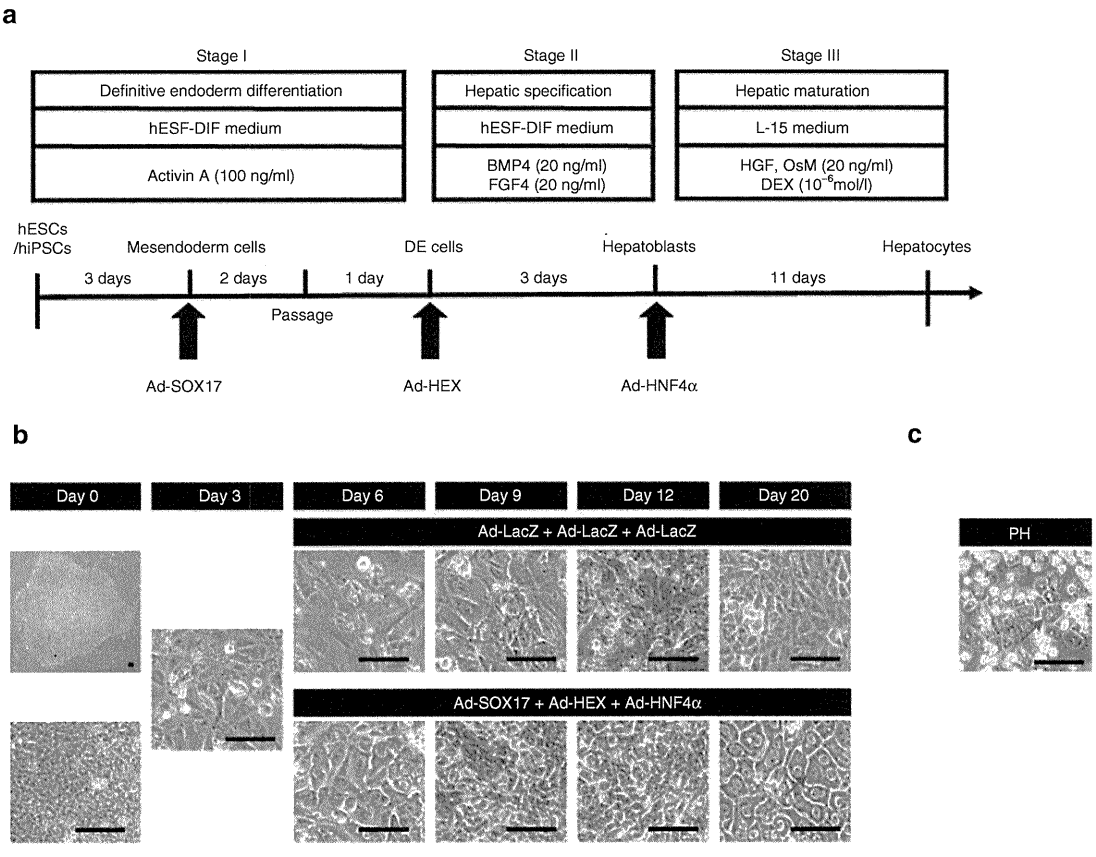

Figure 2 Hepatic differentiation of human ESCs and iPSCs transduced with three factors. (**a**) The procedure for differentiation of human ESCs and iPSCs into hepatocytes via DE cells and hepatoblasts is presented schematically. The hESF-DIF medium was supplemented with 10 μg/ml human recombinant insulin, 5 μg/ml human apotransferrin, 10 μmol/l 2-mercaptoethanol, 10 μmol/l ethanolamine, 10 μmol/l sodium selenite, and 0.5 mg/ml fatty-acid-free BSA. The L15 medium was supplemented with 8.3% tryptose phosphate broth, 8.3% FBS, 10 μmol/l hydrocortisone 21-hemisuccinate, 1 μmol/l insulin, and 25 mmol/l $NaHCO_3$. (**b**) Sequential morphological changes (day 0–20) of human ESCs (H9) differentiated into hepatocytes via DE cells and hepatoblasts are shown. Red arrow shows the cells that have double nuclei. (**c**) The morphology of primary human hepatocytes is shown. Bar represents 50 μm. BSA, bovine serum albumin; DE, definitive endoderm; ESC, embryonic stem cell; iPSC, induced pluripotent stem cell.

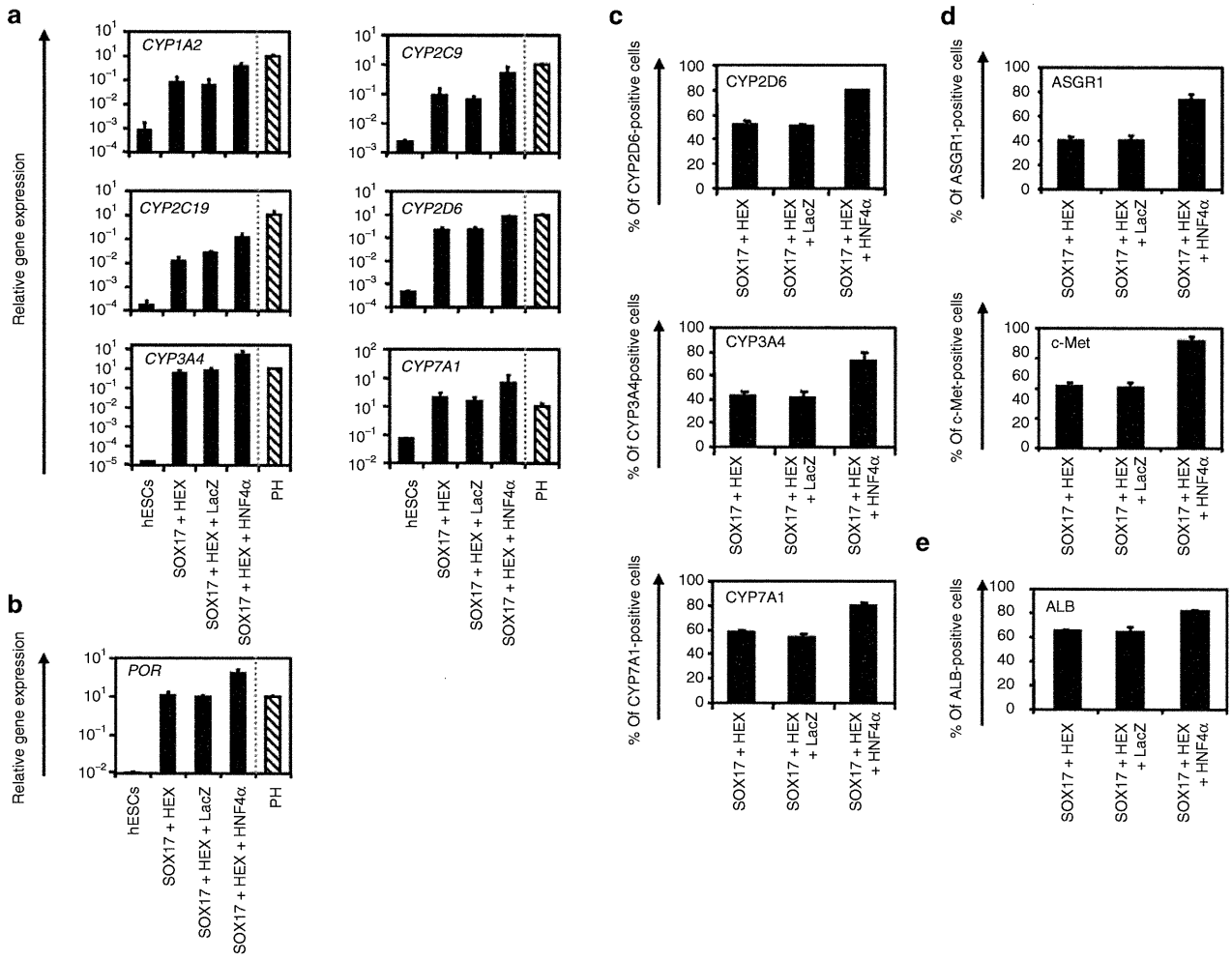

Figure 3 Transduction of HNF4α promotes hepatic maturation from human ESCs and iPSCs. (**a**,**b**) The human ESCs were differentiated into hepatocytes according to the protocol described in **Figure 2a**. On day 20 of differentiation, the gene expression levels of (**a**) CYP enzymes (*CYP1A2*, *CYP2C9*, *CYP2C19*, *CYP2D6*, *CYP3A4*, and *CYP7A1*) and (**b**) *POR* were examined by real-time RT-PCR in undifferentiated human ESCs (hESCs), the hepatocyte-like cells, and primary human hepatocytes (PH, hatched bar). On the y-axis, the expression level of primary human hepatocytes, which were cultured for 48 hours after the cells were plated, was taken as 1.0. (**c**–**e**) The hepatocyte-like cells (day 20) were subjected to immunostaining with (**c**) anti-drug-metabolizing enzymes (CYP2D6, CYP3A4, and CYP7A1), (**d**) anti-hepatic surface protein (ASGR1 and c-Met), and (**e**) anti-ALB antibodies, and then the percentage of antigen-positive cells was examined by flow cytometry on day 20 of differentiation. All data are represented as means ± SD (n = 3). ESC, embryonic stem cell; HNF4α, hepatocyte nuclear factor 4α; iPSC, induced pluripotent stem cell.

(POR)[26], which is required for the normal function of CYPs, was also higher in the three factors-transduced cells (**Figure 3b**). The gene expression analysis of ALB, α-1-antitrypsin (α-1-AT), transthyretin, hepatic conjugating enzymes, hepatic transporters, and hepatic transcription factors also showed higher expression levels in the three factors-transduced cells (**Supplementary Figures S7** and **S8**). Moreover, the gene expression levels of these hepatic markers of three factor-transduced cells were similar to those of primary human hepatocytes, although the levels depended on the type of gene (**Figure 3a,b**, and **Supplementary Figures S7** and **S8**). To confirm that similar results could be obtained with human iPSCs, we used three human iPS cell lines (201B7, Dotcom, and Tic). The gene expression of hepatic markers in human ESC- and iPSC-derived hepatocytes were analyzed by real-time reverse transcription-PCR on day 20 of differentiation. Three human iPS cell lines as well as human ESCs also effectively differentiated into hepatocytes in response to transduction of the three factors (**Supplementary Figure S9**). Interestingly, we observed differences in the hepatic maturation efficiency among the three human iPS cell lines. That is, two of the human iPS cell lines (Tic and Dotcom) were more committed to the hepatic lineage than another human iPS cell line (201B7). Because almost homogeneous hepatocyte-like cells would be more useful in basic research, regenerative medicine, and drug discovery, we also examined whether our novel methods for hepatic maturation could generate a homogeneous hepatocyte population by flow cytometry analysis (**Figure 3c–e**). The percentages of CYP2D6-, CYP3A4-, and CYP7A1-positive cells were ~80% in the three factors-transduced cells, while they were ~50% in the two factors-transduced cells (**Figure 3c**). The percentages of hepatic surface antigen (asialoglycoprotein receptor 1 (ASGR1] and met proto-oncogene (c-Met))-positive cells (**Figure 3d**) and ALB-positive cells (**Figure 3e**) were also ~80% in the three factors-transduced cells. These results indicated that a nearly homogeneous population was obtained by our differentiation protocol

using the transduction of three functional genes (SOX17, HEX, and HNF4α).

The three factors-transduced cells have characteristics of functional hepatocytes

The hepatic functions of the hepatocyte-like cells, such as the uptake of low-density lipoprotein (LDL) and CYP enzymes activity, of the hepatocyte-like cells were examined on day 20 of differentiation. Approximately 87% of the three factors-transduced cells uptook LDL in the medium, whereas only 44% of the two factors-transduced cells did so (**Figure 4a**). The activities of CYP enzymes of the hepatocyte-like cells were measured according to the metabolism of the CYP3A4, CYP2C9, or CYP1A2 substrates (**Figure 4b**). The metabolites were detected in the three factors-transduced cells and their activities were higher than those of the two factors-transduced cells (dimethyl sulfoxide (DMSO) column). We further tested the induction of CYP3A4, CYP2C9, and CYP1A2 by chemical stimulation, since CYP3A4, CYP2C9, and CYP1A2 are the important prevalent CYP isozymes in the liver and are involved in the metabolism of a significant proportion of the currently available commercial drugs (rifampicin or omeprazole column). It is well known that CYP3A4 and CYP2C9 can be induced by rifampicin, whereas CYP1A2 can be induced by omeprazole. The hepatocyte-like cells were treated with either of these. Although undifferentiated human ESCs responsed to neither rifampicin nor omeprazole (data not shown), the hepatocyte-like cells produced more metabolites in response to chemical stimulation as well as primary hepatocytes (**Figure 4b**). The activity levels of the hepatocyte-like cells as compared with those of primary human hepatocytes depended on the types of CYP; the CYP3A4 activity of the hepatocyte-like cells was similar to that of primary human hepatocytes, whereas the CYP2C9 and CYP1A2 activities of the hepatocyte-like cells were slightly lower than those of primary human hepatocytes (**Figure 3a**). These results indicated that high levels of functional CYP enzymes were detectable in the hepatocyte-like cells.

The metabolism of diverse compounds involving uptake, conjugation, and the subsequent release of the compounds is an important function of hepatocytes. Uptake and release of Indocyanine green (ICG) can often be used to identify hepatocytes in ESC differentiation models.[27] To investigate this function in our hepatocyte-like cells, we compared this ability of the three factors-transduced cells with that of the two factors-transduced cells on day 20 of differentiation (**Figure 4c**). The three factors-transduced cells had more ability to uptake ICG and to excrete ICG by culturing without ICG for 6 hours. We also examined whether the hepatocyte-like cells could store glycogen, a characteristic of functional hepatocytes (**Figure 4d**). On day 20 of differentiation, the three factors-transduced cells and the two factors-transduced cells were stained for cytoplasmic glycogen using the Periodic Acid-Schiff staining procedure. The three factors-transduced cells exhibited more abundant storage of glycogen than the two-factors-transduced cells. These results showed that abundant hepatic functions, such as uptake and excretion of ICG and storage of glycogen, were obtained by the transduction of three factors.

Many adverse drug reactions are caused by the CYP-dependent activation of drugs into reactive metabolites.[28] In order to examine metabolism-mediated toxicity and to improve the safety of drug candidates, primary human hepatocytes are widely used.[28] Because primary human hepatocytes have quite different characteristics among distinct lots and because it is difficult to purchase large amounts of primary human hepatocytes that have the same characteristics, hepatocyte-like cells are expected to be used for this purpose. To examine whether our hepatocyte-like cells could be used to predict metabolism-mediated toxicity, the hepatocyte-like cells were incubated with four substrates (troglitazone, acetaminophen, cyclophosphamide, and carbamazepine), which are known to generate toxic metabolites by CYP enzymes, and then the cell viability was measured (**Figure 4e**). The cell viability of the two factors plus Ad-LacZ-tansduced cells were higher than that of the three factors-transduced cells at each different concentration of four test compounds. These results indicated that the three factors-transduced cells could more efficiently metabolize the test compounds and thereby induce higher toxicity than either the two factors-transduced cells or undifferentiated human ESCs. The cell viability of the three factors-transduced cells was slightly higher than that of primary human hepatocytes.

HNF4α promotes hepatic maturation by activating mesenchymal-to-epithelial transition

HNF4α is known as a dominant regulator of the epithelial phenotype because its ectopic expression in fibroblasts (such as NIH 3T3 cells) induces mesenchymal-to-epithelial transition (MET)[11], although it is not known whether HNF4α can promote MET in hepatic differentiation. Therefore, we examined whether HNF4α transduction promotes hepatic maturation from hepatoblasts by activating MET. To clarify whether MET is activated by HNF4α transduction, the human ESC-derived hepatoblasts (day 9) were transduced with Ad-LacZ or Ad-HNF4α, and the resulting phenotype was analyzed on day 12 of differentiation (**Figure 5**). This time, we confirmed that HNF4α transduction decreased the population of N-cadherin (hepatoblast marker)-positive cells,[29] whereas it increased that of ALB (hepatocyte marker)-positive cells (**Figure 5a**). The number of CK7 (cholangiocyte marker)-positive population did not change (**Figure 5a**). To investigate whether these results were attributable to MET, the alteration of the expression of several mesenchymal and epithelial markers was examined (**Figure 5b**). The human ESC-derived hepatoblasts (day 9) were almost homogeneously N-cadherin[30] (mesenchymal marker)-positive and E-cadherin[11] (epithelial marker)-negative, demonstrating that human ESC-derived hepatoblasts have mesenchymal characteristics (**Figure 5a,b**). After HNF4α transduction, the number of E-cadherin-positive cells was increased and reached ~90% on day 20, whereas that of N-cadherin-positive cells was decreased and was less than 5% on day 20 (**Supplementary Figure S10**). These results indicated that MET was promoted by HNF4α transduction in hepatic differentiation from hepatoblasts. Interestingly, the number of growing cells was decreased by HNF4α transduction (**Figure 5c**), and the cell growth was delayed by HNF4α transduction (**Supplementary Figure S11**). This decrease in the number of growing cells might have been because the differentiation was promoted by HNF4α transduction. We also confirmed that MET was promoted by HNF4α transduction in the gene expression levels (**Figure 5d**).

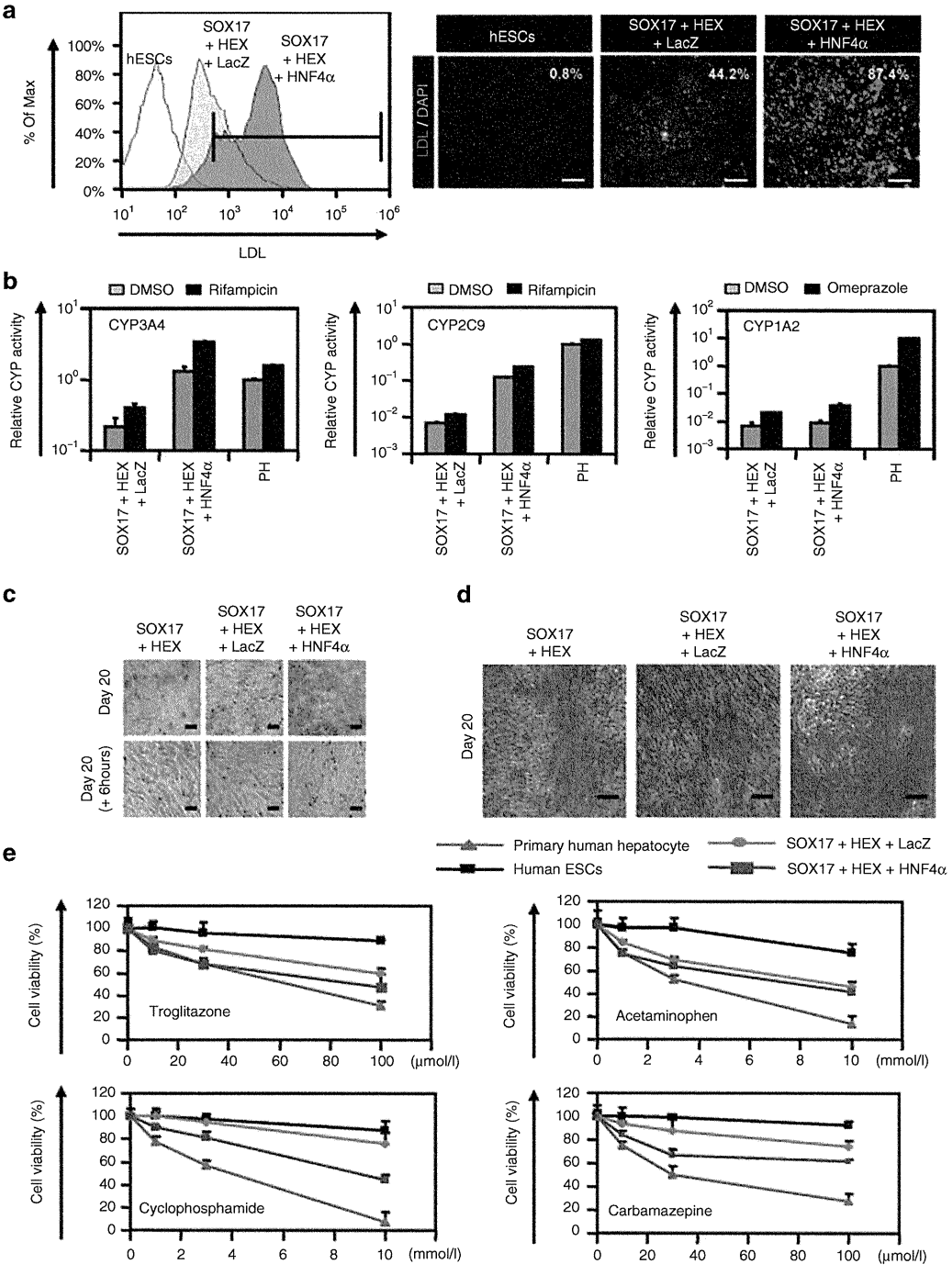

Figure 4 Transduction of the three factors enhances hepatic functions. The human ESCs were differentiated into hepatoblasts and transduced with 3,000 VP/cell of Ad-LacZ or Ad-HNF4α for 1.5 hours and cultured until day 20 of differentiation according to the protocol described in **Figure 2a**. The hepatic functions of the two factors plus Ad-LacZ-transduced cells (SOX17+HEX+LacZ) and the three factors-transduced cells (SOX17+HEX+HNF4α) were compared. (**a**) Undifferentiated human ESCs (hESCs) and the hepatocyte-like cells (day 20) were cultured with medium containing Alexa-Flour 488-labeled LDL (green) for 1 hour, and immunohistochemistry and flow cytometry analysis were performed. The percentage of LDL-positive cells was measured by flow cytometry. Nuclei were counterstained with DAPI (blue). The bar represents 100 μm. (**b**) Induction of CYP3A4 (left), CYP2C9 (middle), or CYP1A2 (right) by DMSO (gray bar), rifampicin (black bar), or omeprazole (black bar) in the hepatocyte-like cells (day 20) and primary human hepatocytes (PH), which were cultured for 48 hours after the cells were plated. On the y-axis, the activity of primary human hepatocytes that have been cultured with medium containing DMSO was taken as 1.0. (**c**) The hepatocyte-like cells (day 20) (upper column) were examined for their ability to take up Indocyanin Green (ICG) and release it 6 hours thereafter (lower column). (**d**) Glycogen storage of the hepatocyte-like cells (day 20) was assessed by Periodic Acid-Schiff (PAS) staining. PAS staining was performed on day 20 of differentiation. Glycogen storage is indicated by pink or dark red-purple cytoplasms. The bar represents 100 μm. (**e**) The cell viability of undifferentiated human ESCs (black), two factors plus Ad-LacZ-tansduced cells (green), the three factors-transduced cells (blue), and primary human hepatocytes (red) was assessed by Alamar Blue assay after 48 hours exposure to different concentrations of four test compounds (troglitazone, acetaminophen, cyclophosphamide, and carbamazepine). The cell viability is expressed as a percentage of cells treated with solvent only treat: 0.1% DMSO except for carbamazepine: 0.5% DMSO. All data are represented as means ± SD ($n = 3$). ESC, embryonic stem cell; DMSO, dimethyl sulfoxide; LDL, low-density lipoprotein.